European Journal of Medicinal Chemistry 203 (2020) 112529

Contents lists available at ScienceDirect

European Journal of Medicinal Chemistry

journal homepage: http://www.elsevier.com/locate/ejmech

Research paper

Chlorine substituents and linker topology as factors of 5-HT$_6$R activity for novel highly active 1,3,5-triazine derivatives with procognitive properties *in vivo*

Sylwia Sudoł [a], Katarzyna Kucwaj-Brysz [a, b], Rafał Kurczab [b], Natalia Wilczyńska [c], Magdalena Jastrzębska-Więsek [c], Grzegorz Satała [b], Gniewomir Latacz [a], Monika Głuch-Lutwin [d], Barbara Mordyl [d], Ewa Żesławska [e], Wojciech Nitek [f], Anna Partyka [c], Kamila Buzun [a, g], Agata Doroz-Płonka [a], Anna Wesołowska [c], Anna Bielawska [g], Jadwiga Handzlik [a, *]

[a] Department of Technology and Biotechnology of Drugs, Faculty of Pharmacy, Jagiellonian University, Medical College, Medyczna 9, PL 30-688, Kraków, Poland
[b] Department of Medicinal Chemistry, Maj Institute of Pharmacology, Polish Academy of Sciences, Smętna 12, PL 31-343, Kraków, Poland
[c] Department of Clinical Pharmacy, Faculty of Pharmacy, Jagiellonian University, Medical College, Medyczna 9, PL 30-688, Kraków, Poland
[d] Department of Pharmacobiology, Faculty of Pharmacy, Jagiellonian University, Medical College, Medyczna 9, PL 30-688, Kraków, Poland
[e] Institute of Biology, Pedagogical University of Cracow, Podchorążych 2, PL 30-084, Kraków, Poland
[f] Faculty of Chemistry, Jagiellonian University, Gronostajowa 2, PL 30-387, Kraków, Poland
[g] Deparmtent of Biotechnology, Medical University of Białystok, PL 15-222, Białystok, Poland

ARTICLE INFO

Article history:
Received 6 April 2020
Received in revised form
14 May 2020
Accepted 1 June 2020
Available online 6 July 2020

Keywords:
Serotonin receptors
5-HT$_6$ antagonist
1,3,5-Triazine
Docking QPLD
Procognitive
Halogen bonds

ABSTRACT

In the light of recent lines of evidence, 5-HT$_6$R ligands are a promising tool for future treatment of memory impairment. Hence, this study has supplied highly potent 5-HT$_6$R agents with procognitive effects, which represent an original chemical class of 1,3,5-triazines, different from widely studied sulfone and indole-like 5-HT$_6$R ligands. The new compounds were rationally designed as modifications of lead, 4-(1-(2-chlorophenoxy)ethyl)-6-(4-methylpiperazin-1-yl)-1,3,5-triazin-2-amine (**1**), involving an introduction of: (*i*) two chlorines at benzene ring and (*ii*) varied linkers joining the triazine ring to aromatic ethers. Synthesis, *in vitro* and *in vivo* biological tests and computer-aided SAR analysis for 19 new compounds were carried out. Most of the new triazines displayed high affinity (K_i < 100 nM) and selectivity towards 5-HT$_6$R, with respect to 5-HT$_{2A}$R, 5-HT$_7$R and D$_2$R. The crystallography-supported docking studies, including quantum-polarized ligand docking (QPLD), indicated that chlorine atoms may be involved in different type of halogen bonding, however, the linker properties seem to predominately affect the 5-HT$_6$R affinity. 4-[1-(2,5-Dichlorophenoxy)propyl]-6-(4-methylpiperazin-1-yl)-1,3,5-triazin-2-amine (**9**), which displayed: the highest affinity (K_i = 6 nM), very strong 5-HT$_6$R antagonistic action (K_B = 27 pM), procognitive effects *in vivo* in novel object recognition (NOR) test in rats, a very good permeability in PAMPA model and satisfying safety *in vitro*, was identified as the most potent 1,3,5-triazine agent so far, useful as a new lead for further research.

1. Introduction

The serotoninergic 5-HT$_6$ receptor was discovered in 1993 as one of the latest members of serotoninergic system [1], being structurally and pharmacologically different from other subtypes [2]. As typical G-protein coupled receptor, it stimulates activity of adenylyl cyclase, which results with cyclic AMP increase. The attractiveness of this receptor as therapeutic target has been growing up since many preclinical studies confirmed an efficacy of the 5-HT$_6$R ligands in serious central nervous system (CNS) dysfunctions, such as: depression [3], Alzheimer's disease (AD) [4,5], schizophrenia [6] and obesity [7,8]. Additionally, very recent

* Corresponding author.
E-mail address: j.handzlik@uj.edu.pl (J. Handzlik).

https://doi.org/10.1016/j.ejmech.2020.112529

research indicated that 5-HT_6R antagonism may be a useful tool in treatment of irritable bowel syndrome (IBS) [9]. Importantly, both the 5-HT_6R antagonist and agonist, were able to improve memory impairment in novel object recognition- (NOR), social recognition- (SRT), Y-maze continuous spontaneous alternation- (Y-CAT) and Morris water maze (MWM) tests in rats [10,11]. This makes 5-HT_6 receptor an intriguing protein target, demanding in-depth research that leads to elucidation of its mechanism of action.

Despite of a number of already synthesized and pharmacologically evaluated 5-HT_6R ligands, none has been approved as new drug in pharmaceutical market. Several 5-HT_6R agents have reached clinical trials (Fig. 1) [12–17] but, for the time being, the clinical experiments have not confirmed clearly either significant procognitive effects in patients with mild to severe AD or anxiolytic ones in patients with schizophrenia, thus highlighting a need of further studies on 5-HT_6R-mediated mechanisms of action. Worth noting, the majority of previously found 5-HT_6R ligands, belongs mainly to two chemical classes, *i.e.*: indole-derivatives or sulfones [18]. Given all the mentioned-above facts, a further search for chemically original 5-HT_6R agents, which could be translated into efficacy in clinical trials, seems to be relevant in terms of rational strategy for new potential treatment of CNS disorders.

On the other hand, halogen atoms are substituents very widely used in medicinal chemistry as their introduction into molecules often results in an improvement of metabolic stability [19], blood-brain barrier (BBB) penetration [20] or other biological membrane permeability [21]. Moreover, their presence may provide higher activity thanks to ability to form non-covalent interactions, so-called halogen bonding (XB), thus stabilizing protein-ligand complex [22]. The importance of this phenomena has been already confirmed in search for 5-HT_6R antagonists [23], but also for ligands of other GPCRs (*e.g.* 5-HT_{1A} [24], 5-HT_{2B}R [25], 5-HT_7R [26], D_2R, D_4R [27]). Taking into account aforementioned facts, halogen substituents can be considered as those of the first order in pharmacomodulation of novel biologically active small molecules.

Intending to explore a new chemical space for 5-HT_6R ligands, our recent research was concentrated on design, synthesis and pharmacological characteristics of novel, non-indole and non-sulfone, family of 1,3,5-triazine derivatives to give a group of new 5-HT_6R agents with high affinity (K_i < 100 nM) and selectivity for 5-HT_6 receptor [28–31]. The structure-activity relationship (SAR) analysis for those 1,3,5-triazine 5-HT_6R ligands showed a significant role of their linker and a linker-dependent substitution in the aromatic system. Thus, the lipophilic substituent in *meta* position was conducive to activity in the series of 1,3,5-triazines with the methylene linker [31]. In the case of the cyclic moiety in the linker, *para* substitution was the most advantageous [29], while compounds containing an ether linker were found as the most interesting group, giving broad possibilities for further modifications [28,30,32]. In that last group, compound **MST4,** containing alkyl substituents at both, 2- and 5-positions of benzene, was the most active derivative found so far (K_i = 11 nM, Fig. 2) [32]. It is worth to underline, that alkyl mono-substituted (at the benzene ring) analogues of **MST4** were significantly less active (K_i = 87–235 nM), while better results were observed for some chlorine mono-substituted derivatives. Among them, compound **WA-13** (**1,** Fig. 2), containing *o*-chlorobenzene and the methyl branching linker took our special attention, as displaying both potent (K_i = 23 nM) and selective action on 5-HT_6R as well as satisfying CNS-druglike properties. Furthermore, antidepressant effect of **1** was confirmed in the forced swim test (FST) in rats [28]. In this context, the compound **1** was selected as an appropriate lead structure for further chemical modifications.

Therefore, this study was focused on design, synthesis and biological evaluation of novel derivatives of the lead **1**, where the main chemical modifications concerned a variety of chlorine di-substitutions at the phenyl aromatic ring (R^1). Furthermore, modifications of the linker, *i.e.* length (n) and branching (R^2), were carried out (Fig. 2). In term to complete SAR analysis, one compound with the unsubstituted phenyl ring, but branched linker, was under consideration.

For this purpose, synthesis of 19 new derivatives of **WA-13** (**2**–**20**, Fig. 2) has been performed. Whole the series (**2**–**20**) was tested for the affinity and selectivity towards 5-HT_6R in the radioligand binding assay (RBA). Selected active compounds have been evaluated in extended screening, including: (i) their intrinsic activity in functional assays, (ii) ADMETox properties *in vitro* as well as (iii) behavioral tests *in vivo*. In order to perform comprehensive SAR analysis, crystal structures for two representative members with different length of linkers have been carried out, followed by molecular modelling, including quantum-polarized ligand docking (QPLD), with special emphasize on role of halogen bond in ligand-receptor complexes.

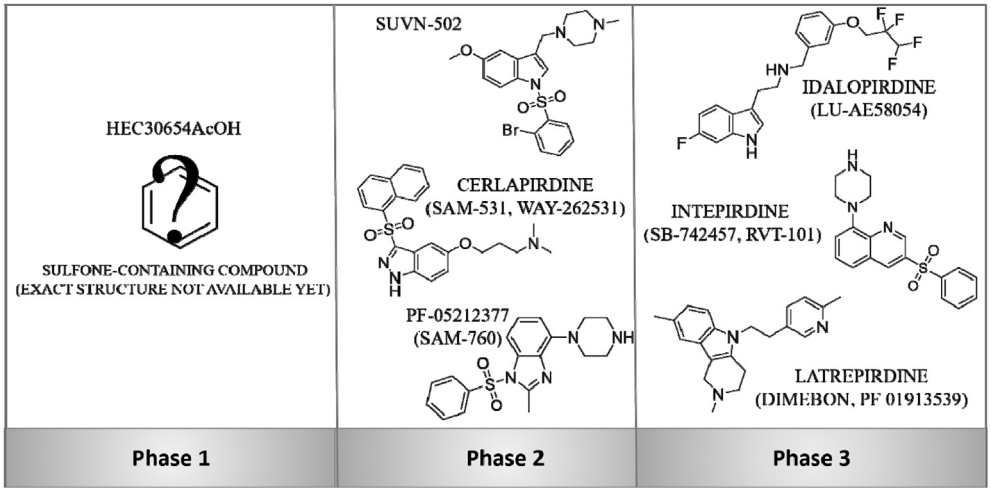

Fig. 1. The 5-HT_6R antagonists, which reached clinical trials.

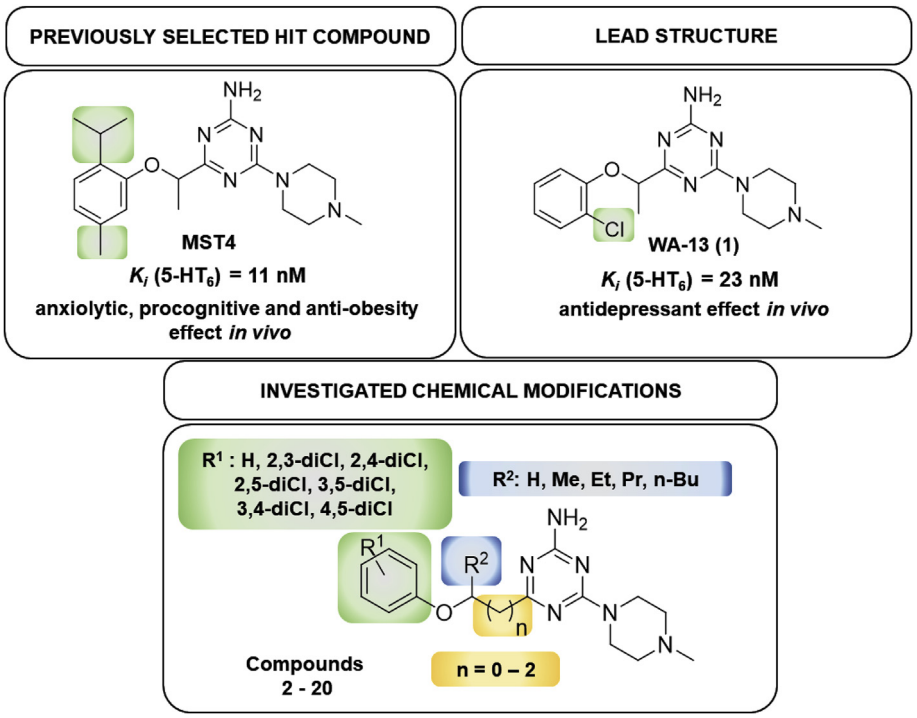

Fig. 2. The previously reported hit compound (**MST4**), the lead structure (**WA-13**, **1**) and its chemical modifications investigated within this study.

2. Results

2.1. Synthesis

The compounds (**2**–**20**) were obtained within 2-step synthesis pathways, elaborated on the basis of procedures described for previous 1,3,5-triazines [13]. In the first step, O-alkylation of commercial (dichloro)phenols with appropriate bromoesters was used to give aromatic ethers (**22**–**40**). Then, the cyclic condensation of 4-methylpiperazin-1-yl biguanide dihydrochloride (**21**) with the adequate ester (**22**–**40**) was carried out to form a 1,3,5-triazine ring resulting in final products **2**–**20** (Scheme 1). As the racemic mixtures of bromoesters were applied for the synthesis of the aromatic ethers (**22**–**26**, **28**–**31**, **33**, **34**, **36**–**39**), consequently racemic mixtures of the final compounds (**2**–**6**, **8**–**11**, **13**, **14**, **16**–**19**) were obtained.

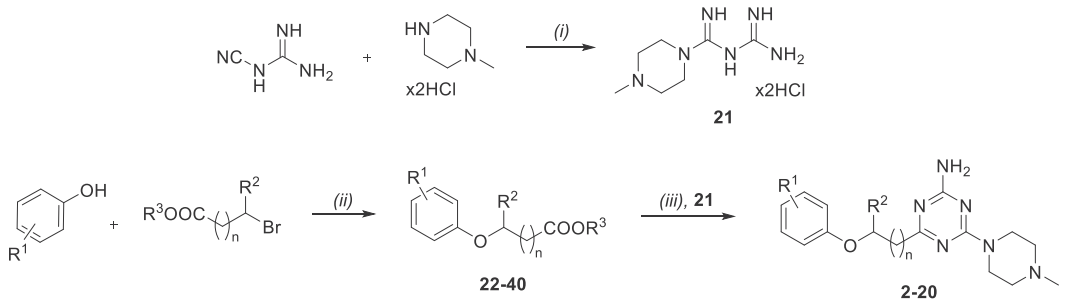

22: R^1 = H; R^2 = Et; R^3 = Me
23: R^1 = 2,3-diCl; R^2 = Me; R^3 = Me
24: R^1 = 2,3-diCl; R^2 = Et; R^3 = Me
25: R^1 = 2,3-diCl; R^2 = Pr; R^3 = Et
26: R^1 = 2,3-diCl; R^2 = n-Bu; R^3 = Et
27: R^1 = 2,3-diCl; R^2 = H; R^3 = Et
28: R^1 = 2,5-diCl; R^2 = Me; R^3 = Me
29: R^1 = 2,5-diCl; R^2 = Et; R^3 = Me
30: R^1 = 2,5-diCl; R^2 = Pr; R^3 = Et
31: R^1 = 2,5-diCl; R^2 = n-Bu; R^3 = Me
32: R^1 = 2,5-diCl; R^2 = H; R^3 = Et
33: R^1 = 3,4-diCl; R^2 = Me; R^3 = Me
34: R^1 = 4,5-diCl; R^2 = Et; R^3 = Me
35: R^1 = 4,5-diCl; R^2 = H; R^3 = Et
36: R^1 = 3,5-diCl; R^2 = Me; R^3 = Me
37: R^1 = 3,5-diCl; R^2 = Et; R^3 = Me
38: R^1 = 3,5-diCl; R^2 = Pr; R^3 = Et
39: R^1 = 3,5-diCl; R^2 = n-Bu; R^3 = Me
40: R^1 = 2,4-diCl; R^2 = H; R^3 = Et

Scheme 1. Synthetic route for compounds **2**–**20**. Reagents and conditions: (*i*) BuOH, reflux, yield: 86%; (*ii*) acetonitrile, K_2CO_3, reflux, 2–16 h, yield: 36–90%; (*iii*) absolute methanol, Na, reflux 15–30 h, yield: 13–52%.

Table 1
Radioligand binding assays results for the newly synthesized compounds **2**–**20**.

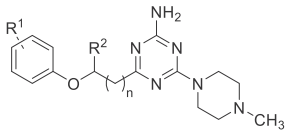

2-20

Compound	R^1	R^2	n	*Ki* [nM][a]			
				5-HT_6	5-HT_{2A}	5-HT_7	D_2
Lead 1	2-Cl	Me	0	23	1830	38730	1001
2	H	Et	0	**21**	5047	19940	1506
3	2,3-diCl	Me	0	**16**	268	12550	432
4	2,3-diCl	Et	0	**6**	209	5202	421
5	2,3-diCl	Pr	0	**23**	310	13420	495
6	2,3-diCl	n-Bu	0	**73**	470	5265	506
7	2,3-diCl	H	2	**274**	649	8592	206
8	2,5-diCl	Me	0	**13**	355	15050	375
9	2,5-diCl	Et	0	**6**	484	5706	320
10	2,5-diCl	Pr	0	**12**	382	12470	229
11	2,5-diCl	n-Bu	0	**17**	431	6263	103
12	2,5-diCl	H	2	**470**	1457	7924	413
13	3,4-diCl	Me	0	**95**	576	5928	754
14	3,4-diCl	Et	0	**86**	696	5098	580
15	3,4-diCl	H	2	**1061**	906	4879	356
16	3,5-diCl	Me	0	**27**	412	9398	157
17	3,5-diCl	Et	0	**11**	463	9483	368
18	3,5-diCl	Pr	0	**26**	488	19850	377
19	3,5-diCl	n-Bu	0	**51**	839	10880	270
20	2,4-diCl	H	2	**999**	nt[c]	1904	nt[c]
Ref[b]	–	–	–	**7**			9

[a] The standard deviation values are reported in Supplementary materials, Table S2.
[b] Olanzapine.
[c] nt – not tested.

2.2. Pharmacology in vitro

2.2.1. Radioligand binding assays

The binding affinities for all the newly synthesized 1,3,5-triazine derivatives **2**–**20** towards the 5-HT_6 receptor and competitive ones, *i.e.* serotoninergic receptors 5-HT_{2A}, 5-HT_7 and dopaminergic D_2 receptor, have been assessed in radioligand binding assays (Table 1).

Serotonin 5-HT_{2A}R and dopaminergic D_2R were chosen as protein off-targets in order to control interactions which might be responsible for undesired side effects. According to literature, activation of 5-HT_{2A}R leads to hallucinations [33], whereas interaction with D_2R is associated with extrapyramidal symptoms (*e.g.* acute dystonia and parkinsonian symptoms) [34]. Additionally, studies on animal models showed that 5-HT_7R ligands may cause procognitive effects [35], similarly as 5-HT_6R agents. In order to clarify, if herein investigated procognitive effects are a result of interaction with 5-HT_6R, the 5-HT_7R was also selected as competitive protein target.

According to results obtained, most of the triazine compounds (**2**–**6**, **8**–**11**, **13**, **14** and **16**–**19**) showed high affinity for 5-HT_6R (K_i < 100 nM) and significant selectivity, with respect to other GPCR's. Ten compounds were more potent than lead structure **WA-13** (K_i < 23 nM). Compounds **4** and **9** turned out to have the highest 5-HT_6R affinity (K_i = 6 nM), in 2-fold more potent than the most active triazine 5-HT_6R ligand described so far (**MST4**, K_i = 11 nM) [18]. Compound **2** demonstrated the most significant selectivity towards 5-HT_6R, with respect to the rest of considered receptors (5-HT_{2A}R: 240-fold, 5-HT_7R: 950-fold, D_2R: 72-fold).

2.2.2. Functional assays towards 5-HT_6 receptor

Selected active compounds (**3**, **8**, **9**, **11** and **16)** were tested in the functional assays, in order to study their intrinsic activity towards 5-HT_6R. During the experiments, the level of cAMP was measured (Table 2).

None of the tested derivatives showed agonistic mechanism, while four out of them showed strong antagonistic action in the low nanomolar- (**3**, **8**, **16**) or even picomolar range in the case of **9** (pK_B = 10.57, *i.e.* K_B = 27 pM, Table S3, Supplementary).

2.3. Drug-likeness in vitro

2.3.1. Permeability

For active representatives of the novel triazine derivatives, **8** and **9,** permeability was tested using Parallel Artificial Membrane Permeability Assay (PAMPA). The test is based on compounds' passive penetration through the bilayer artificial membranes. This membrane may imitate barriers for compound absorption from the intestines with a good correlation to *in vivo* conditions. The assay was performed in accordance to previously described methods [36–40]. Both tested ligands (**8** and **9**) had a high permeability coefficient (Pe), higher than that for **MST4** [32] and compared to Pe estimated for caffeine, the reference high-permeable compound (Table 3).

2.3.2. Metabolic stability

The metabolic stability was investigated *in vitro* by using rat liver microsomes (RLMs) and supported with MetaSite 6.01 software. The most probable structures of metabolites were determined. *In silico* predicted sites of metabolism for both compounds **8** and **9** were specified for *N*-methylpiperazine moiety and *para* position of the chlorine di-substituted aromatic ring (Fig. 3).

The incubation with RLMs for 120 min resulted in the formation of six (**9**) or seven (**8**) metabolites, and more than 90% of each compound was biotransformed (Table S1; Fig. 4A and B). Obtained results indicated rather low metabolic stability for both compounds, lower than that for **MST4** [32,41], while **9** was almost in 3-fold more stable than **8** (8.93% of **9** *vs.*3.17% of **8,** remained in the reaction mixture).

These studies allowed us to predict the most probable metabolic pathway, *i.e.* the hydroxylation at the phenyl ring (the metabolite M1), while other probable metabolic pathways included demethylation and hydroxylation of piperazine ring, which were found for both the 5-HT_6R ligands (**8**, **9**) by MS analyses (Table S1; Figs. S1A–G, Figs. S2A–F, Supplementary).

2.3.3. Toxicity

The safety profile of the 1,3,5-triazine derivatives (**8**, **9**) was estimated in the hepatotoxicity assay *in vitro* using *hepatoma* HepG2 cell line, according to the protocol reported earlier [37–40]. Both tested compounds **8** and **9** demonstrated a weak hepatotoxicity effect compared to the used reference toxins (doxorubicin and 3-chlorophenyl-hydrazone). The statistically significant decrease in cells viability was observed only at the highest applied concentration of compound **8** (100 μM, Fig. 5). Compound **9**, due to partial precipitation at 50 and 100 μM, could be correctly tested only at lower concentrations, showing no toxicity up to 10 μM, inclusively. Hence, both compounds (**8**, **9**) displayed a satisfied safety in the level corresponding to the best derivatives of 1,3,5-triazines tested previously [28,31,32,38].

2.4. Behavioral studies in vivo

Taking into account that various previously studied 5-HT_6 receptor ligands, especially antagonists, exhibited beneficial effects

Table 2
The results from functional assays for compounds **3**, **8**, **9**, **11** and **16**.

Compound	Binding affinity pK_i[a]	Antagonist mode pK_B[b] ± SEM	Agonist mode E_{max} [%][c] ± SEM
SEROTONIN	–	N.C.[d]	100 ± 2.0
SB258585	–	8.68 ± 0.055	4 ± 0.5
MIANSERIN	–	6.28 ± 0.023	4 ± 0.0
3	7.80	8.24 ± 0.317	4 ± 0.0
8	7.89	8.44 ± 0.138	6 ± 0.5
9	8.22	10.57 ± 0.065	4 ± 0.0
11	7.77	6.36 ± 0.031	4 ± 0.0
16	7.57	8.78 ± 0.332	11 ± 0.5

[a] Calculated according to the data from Table 1.
[b] Results were normalized as percentage of reference antagonist (SB258585 10^{-5} M).
[c] Results were normalized as percentage of maximal agonist response (serotonin 10^{-5} M); E_{max} is the maximum possible effect.
[d] N.C. - not calculable. The full data with standard deviation values are presented in Supplementary materials, Table S3.

Table 3
Permeability coefficient of compounds **8** and **9.**

Compound	Pe[a] [10^{-6} cm/s] ± SD
8	18.0 ± 1.2
9	18.9 ± 0.9
MST4	12.3 ± 2.0
Reference	Caffeine 15.1 ± 0.4

[a] tested in triplicate.

on cognition in animal models [39], the most active 5-HT_6R antagonist in this study, compound **9**, has been investigated in two models of the memory impairment tests, *i.e.* NOR and NOL (Novel Object Location) tests. Compound SB-742457, the potent 5-HT_6R antagonist with the confirmed ability to reverse MK-801-induced memory impairment in NOR test after both, acute and chronic administrations [10] was used as reference (Fig. 6). The compound **9** dose-depend ameliorated the memory impairment induced by MK-801 (0.1 mg/kg), in the statistically significant manner at the dose of 3 mg/kg (Fig. 6a). The obtained data of discrimination index for the triazine derivative **9** at the dose of 3 mg/kg are comparable with those for the reference SB-742457 at the same dose used (Fig. 6a). Despite, we did not observe any activity of this compound (**9**) in the NOL test (Fig. 6b).

Thus, the improvement of memory was observed only in the case of the memory for objects (what) in the NOR but not in the spatial location (where) in the NOL test. A deficit in episodic memory is one of the well-established cognitive deficits in schizophrenic patients and it is the most profound and earliest cognitive deficit in AD [42]. The improved novel object recognition task, but not the novel location place object preference task, demonstrates dissociation between the effects of the investigated compound in a spatial location (NOL test) and the object recognition (NOR test) version of animal model of episodic memory task. As this dissociation was obtained using identical stimulus types, arena, and identical retention delays of 1 h, it cannot be accounted for by differences in the response requirements of the procedures or attentional or motivational processes. At this stage of our research, it is difficult to explain this loss of activity of compound **9** in NOL test. We can only suppose that this compound at the range of doses used, may possesses ability rather to reverse memory impairment in recognition than in spatial memory components of episodic memory, but it needs extended investigations in the future.

2.5. The computer-aided structure-activity relationship analysis

In order to support structure-activity relationship discussion, in-depth inside into 3D-structure of the investigated compounds (**2**–**20**) and their interactions with target 5-HT_6R protein in the molecular level were performed, including both experimental crystallography and molecular modelling.

2.5.1. Crystallographic studies

Crystallographic analyses for compounds, representing either the shortest (**9**) or the longest (**20**) linker structural category, were carried out giving a starting point to find active conformations for the whole series (**2**–**20**) within molecular modelling studies.

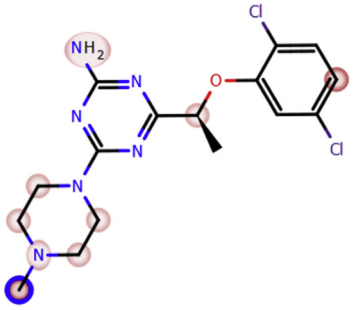

8

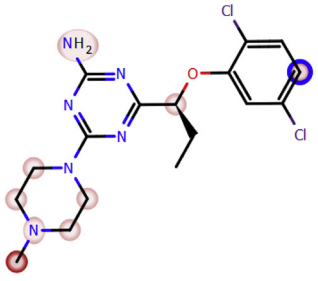

9

Fig. 3. *In silico* prediction of the sites of metabolism by MetaSite 8.0.1 for **8** and **9**. Blue circle marked on the functional group structures indicates the highest biotransformation probability. The fading red color shows the decreasing of the metabolism probability. (For interpretation of the references to color in this figure legend, the reader is referred to the Web version of this article.)

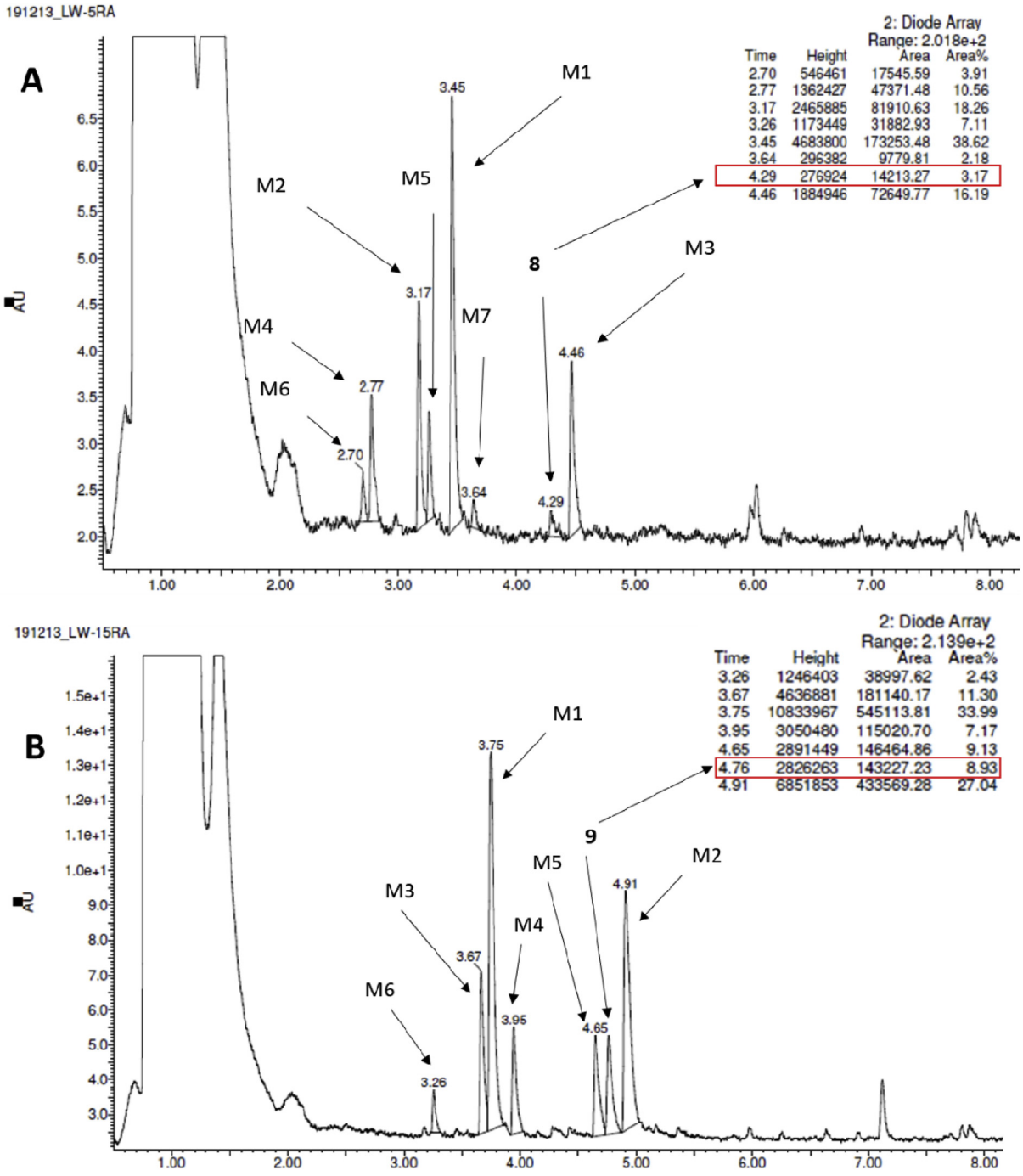

Fig. 4. The UPLC spectra of **8** (A) and **9** (B) and metabolites obtained after 120 min reaction with RLMs.

The overall shapes of the **9** and **20** molecules with the atom-numbering schemes are presented in Fig. 7. Both molecules are isomers possessing the 2-amine-4-(4′-methylpiperazin-1′-yl)-1,3,5-triazine moiety, as well as a di-substituted aromatic ring (2,5-dichloro for **9** and 2,4-dichloro for **20**) connected with the triazine ring by the ethylmetoxylene linker for **9** and the propoxylene linker for **20**. In both molecules the piperazine ring adopts chair conformation with equatorial position of the methyl group. However, the substituent at the N2 atom is not in a typical equatorial position with a torsion angle C4—N2—C7—C8 of about 180°. The values of this angle are 111.1(1)° and 133.8(1)° for **9** and **20**, respectively. These values are lower than in other three crystal structures containing the 2-amine-4-(4′-methylpiperazin-1′-yl)-1,3,5-triazine moiety [43,44] but similar to one observed in the crystal structure of the 2-amine-6-(5-chloro-2-methoxyphenyl)-4-(4′-methylpiperazin-1′-yl)-1,3,5-triazine [43], as well as similar to these observed in the crystal structures of 2-(4-methylpiperazin-1-yl)-1*H*-imidazol-5(4*H*)-one derivatives [45]. The mutual orientation of three rings differs in presented crystal structures. The interplanar angles between triazine and piperazine rings are 43.30(5)° and 28.65(5)°, while between triazine and aromatic rings are 81.50(4)° and 76.62(3)° for **9** and **20**, respectively.

The intermolecular interactions are similar in both structures. The main motif of interactions is based on the N—H···N hydrogen

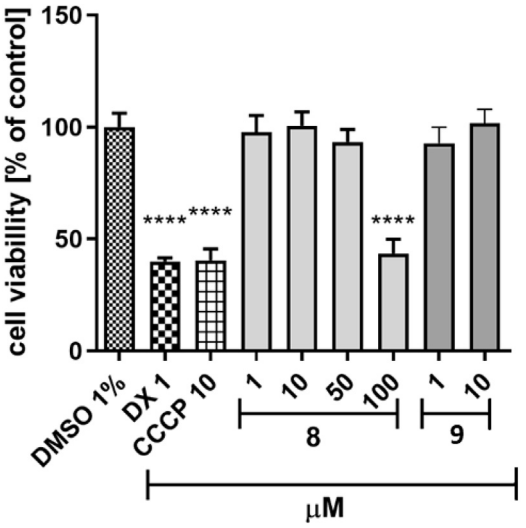

Fig. 5. The effect of tested compounds **8**, **9** and references: doxorubicin (DX, 1 μM), mitochondrial toxin carbonyl cyanide 3-chlorophenyl-hydrazone (CCCP, 10 μM) on *hepatoma* HepG2 cell line viability. Compound **9** partly precipitated at 50 and 100 under assay conditions. 1% DMSO in cell growth media was used as a negative control. GraphPad Prism 8.0.1 was used to calculate the statistical significances by one-way ANOVA, followed by Bonferroni's comparison test (****p < 0.0001, **p < 0.01).

bonds (Fig. 8). These interactions lead to formation of the dimers. In addition, the crystal structures are stabilized by N—H···Cl and C—H···π contacts.

2.5.2. Molecular modelling

The molecular docking study for the newly synthesized derivatives **2**—**20** to 5-HT_6 receptor homology models showed coherent binding mode with the previously reported 1,3,5-triazine derivatives [28—31,41]. The crucial interactions are the salt bridge between protonated methylpiperazine nitrogen and negatively charged D3.32 side chain, an aromatic CH...π or π...π interaction with F6.52 and/or F6.51, and hydrogen bond between NH_2 group of 1,3,5-triazine ring and carbonyl oxygen of V3.33 and/or A5.42. Substituted aromatic fragment linked with the 1,3,5-triazine ring interacted with the hydrophobic cavity formed by transmembrane domains (TM) 3—5 and extracellular loop 2 (ECL2), moreover, its positioned into this cavity is caused by the tetrahedral conformation of the linker. In the light of the molecular docking results, the comparison of the most active derivative **9** with the lead structure **1** (Fig. 9A) showed a retaining of a common binding mode. However, elongation of the linker caused a decrease of activity, which is in line with the molecular docking study. For instance, a comparison of binding modes (Fig. 9A) of compound **9** (K_i = 6 nM) *vs.* **12** (K_i = 470 nM) showed that too long linker may lead to destabilization of the complex and breaking some key interactions (*e.g.* with A5.42/V3.33).

The branching of the linker showed increase of the affinity in order methyl < ethyl, but decrease in order propyl > butyl for each of the compared series. Molecular docking indicated (Fig. 9B) that the branching alkyl group was placed into a small binding cavity formed by helices 5 and 6, which increased the stability of the resulting ligand—receptor complexes for shorter, and destabilized the complexes (perhaps because of the overfilling of this pocket) for the longer branching group.

In term to investigate the role of different substitution of chlorine atoms in the phenyl fragment, the docking procedure involves quantum-polarized ligand docking (QPLD) and the MM/GBSA algorithm was used. This procedure showed better performance in reproducing the X-ray geometries of protein—ligand complexes with halogen bonding than classical docking approach [46], and was also used to the study of the halogen bonding with privileged amino acids as an important factor modulating the activity to 5-HT_6 receptor [29,47]. The disubstituted series, including: 2,3-diCl (**4**), 3,5-diCl (**17**), 2,5-diCl (**9**), and 3,4-diCl (**14**) derivatives, and also the unsubstituted analog (**2**) in the phenyl fragment (Fig. 9C), was selected.

It was possible to calculate the changes in the L—R binding free energy resulting from the substitution of halogen atoms in this fragment (ΔΔG). Analysis of the binding modes showed that

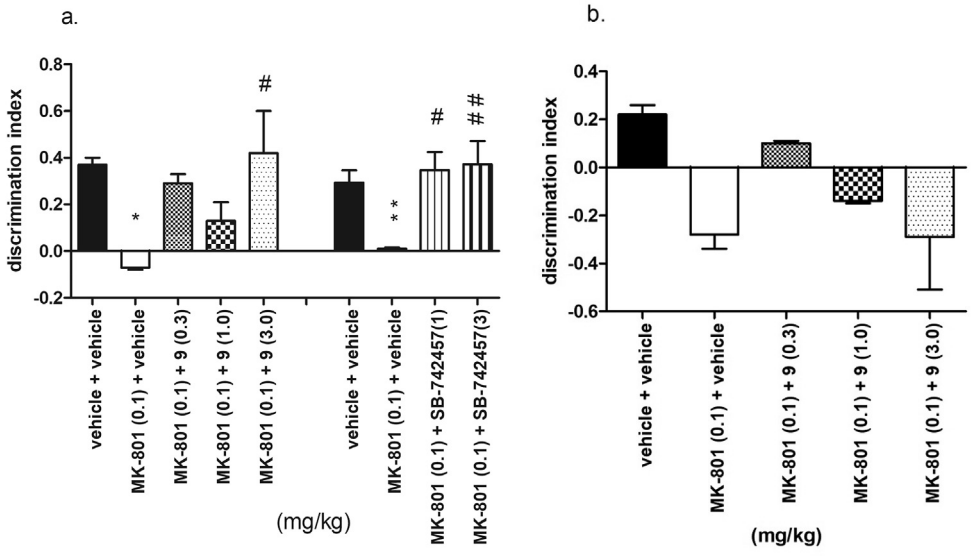

Fig. 6. Effects of compound **9** on the memory impairment induced by MK-801 in NOR (a) and NOL (b) tests. Compound **9** and SB-742457 were administered *i.p.* 60 min, while MK-801 30 min before the T1 session. The animals were observed for 5 min. The data are presented as the mean ± SEM of 6—8 rats. The data were statistically evaluated by one-way ANOVA followed by Bonferroni's post-hoc test,*p < 0.05,**p < 0.01 vs respective vehicle-treated group, and #p < 0.05, ##p < 0.01 vs respective MK-801-treated group. (one-way ANOVA for discrimination index for NOR test: F(4,30) = 3.99, p < 0.01 (for compound **9**) and F(3,40) = 6.78, p < 0.001 (for SB-742457); and for NOL test: F(4,29) = 2.82, p < 0.05).

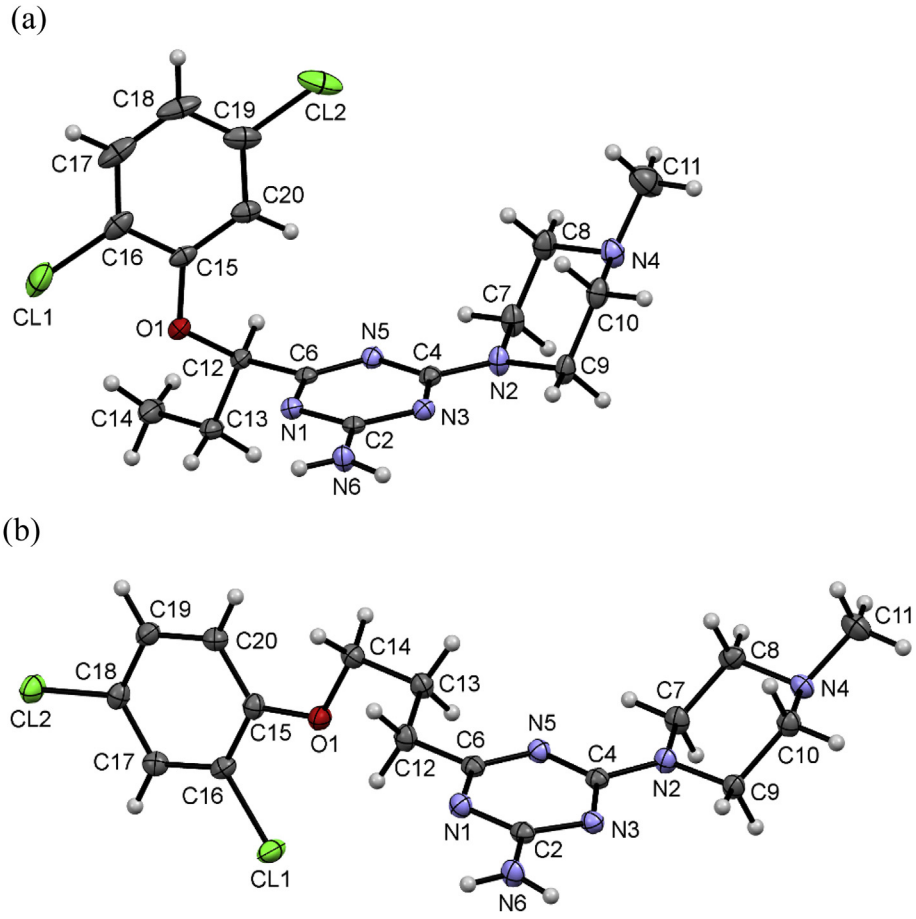

Fig. 7. The molecular structures of (a) **9** and (b) **20**, showing the atom-numbering schemes. Displacement ellipsoids are drawn at the 50% probability level.

chlorine atoms were involved in the formation of different types of halogen bonds (all with backbone carbonyl oxygen), which were also visible in the change of binding free energy and activity of a given derivative. The highest increase of the binding free energy was noted for the most active derivatives **4** and **9** ($K_i = 6$ nM). The first analogue (2,3-diCl) showed $\Delta\Delta G = -2.89$ kcal/mol and two halogen bonds with P4.60 (XB distance = 4.1 Å, σ-hole angle = 165°) and A4.56 (XB distance = 3.0 Å, σ-hole angle = 141°, with chlorine in position 2). The second derivative (2,5-diCl) displayed $\Delta\Delta G = -1.96$ kcal/mol and halogen bonds with A4.56 (XB distance = 2.8 Å, σ-hole angle = 148°) formed by chlorine in position 2, and surprisingly, with L162 from extracellular loop 2 (XB distance = 2.7 Å, σ-hole angle = 162°). The 3,5-diCl analogue **17** showed only slightly lower increase of binding free energy compared to 2,5-diCl ($\Delta\Delta G = -1.78$ kcal/mol), for which two halogen bonds were found as well – with S4.57 (XB distance = 3.8 Å, σ-hole angle = 161°), and with L162 (XB distance = 2.9 Å, σ-hole angle = 152°) formed by chlorine in position 5 (as in the 2,5-diCl derivative). The last derivative **14** (3,4-diCl) showed the lowest increase of binding free energy equal −0.73 kcal/mol, and only one halogen bond was formed between chlorine in position 3 with S4.57 (XB distance = 3.0 Å, σ-hole angle = 172°), whereas the chlorine at position 4 did not show any specific interaction with the binding site. This analysis demonstrated that chlorine atoms may be involved in the formation of halogen bonding, additionally stabilizing the L–R complex, but their contribution is rather moderate (the highest improvement in activity after chlorine substitution is approximately 4-fold).

2.5.3. General SAR discussion

The chemical modifications of the lead **1** were introduced to analyze an influence on the affinity towards 5-HT_6R of two following structural factors: (i) dichloro-substitution at phenyl ring and (ii) the diverse (un)branched linker. The results obtained within this study allow us to perform comprehensive structure-activity relationship discussion.

Sixteen out of nineteen newly synthesized compounds demonstrated a high affinity for 5-HT_6R, with K_i values lower than 100 nM. The best pharmacological activity profile was observed for 2,5- and 2,3-dichlorophenoxy 1,3,5-triazine derivatives with a short but branched alkoxy linker, *i.e.* compounds **4** ($K_i = 6$ nM) and **9** ($K_i = 6$ nM). Both compounds had higher affinity for 5-HT_6R than reference olanzapine as well as the strong picomolar antagonistic action, found for the 2,5-dichlorophenyl derivative **9** ($K_B = 0.027$ nM), is worth emphasizing. Among the series of analogues with chlorine atoms at the same positions of phenyl ring, a change of branching in linker, from methyl to ethyl group, increased the 5-HT_6R affinity, simultaneously maintaining significant selectivity. However, further elongation of branching did not improve activity, giving the least beneficial effects for the butyl group, which is consistent with molecular docking results. The mentioned-above results, together with the high 5-HT_6R affinity ($K_i = 21$ nM) of the compound unsubstituted at the aromatic ring (**2**), indicate that the type of linker is the predominant structural factor for the 5-HT_6R activity of the compounds investigated within this study. This conclusion may be also supported by previous results, in which the unbranched analogue of **2** displayed significantly lower affinity for

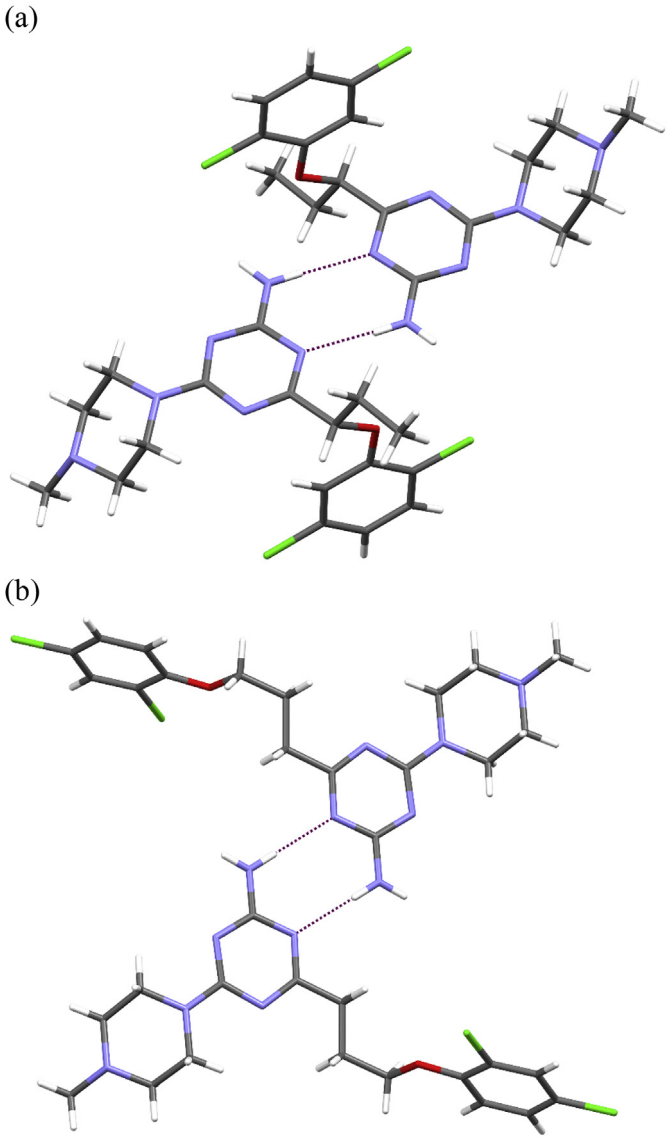

Fig. 8. The dimers in the crystal structure of **9** (a) and **20** (b). Dashed lines indicates the hydrogen bonds.

the 5-HT$_6$R target (K_i = 507 nM) [29]. Additionally, molecular modelling studies confirmed that chlorine atoms might be involved in stabilization of L–R complex through the different type of halogen bonds, however, their effect on the activity improvement is moderate. These results allow to fully explain the high and little-varied activity of branched derivatives *ortho*-, *meta*- or unsubstituted at the phenyl ring.

On the other hand, the presence of two chlorine substituents at the phenyl ring was found as profitable also for "drug-like" properties of the explored 1,3,5-triazines due to an increase of lipophilicity. The higher lipophilicity seems to be desirable to penetrate membrane barriers, including BBB, which is especially important in the case of compounds destined to act on CNS. The representative 2,5-dichlorophenyl derivatives tested (**8**, **9**) demonstrated high permeability (Pe about 18 × 10^{-6} cm/s) and rather low risk of hepatotoxicity in the studies *in vitro*.

Despite the low metabolic stability *in vitro*, the significant procognitive effect of the 2,5-dichlorophenyl derivative **9** *in vivo* was observed in the NOR test in rats. Furthermore, the active dose of **9** was corresponding to that of compounds **MST4** tested previously, although the metabolic stability of **MST4** was in 6-fold higher (59.25% *vs.* 8.93%), and the 5-HT$_6$R affinity only slightly weaker (11 nM *vs.* 6 nM) [32]. The observed procognitive action of compound **9** *in vivo* seems to be a result of combined factors, *i.e.* (i) the beneficial effects of both the highly potent 5-HT$_6$R-antagonistic action and a putative very good blood-brain barrier penetration (high permeability confirmed in PAMPA test) on one hand, but (ii) an unfavorable low metabolic stability effect, on the other. In this context, the resultant effect indicates a distinctly greater impact of those favorable factors. Otherwise, the significant activity in the behavioral test (NOR) could be also caused by synergistic procognitive action of either the compound **9** or the metabolites formed. However, these hypotheses need wider pharmacological and ADMET considerations to be enough confirmed.

3. Conclusions

The described herein novel series of 1,3,5-triazine derivatives enlarged the original family of highly potent 5-HT$_6$R antagonists, structurally different from widely investigated sulfone and indole-like compounds. In particular, the systematic modifications of *o*-chloro substituted lead (**1**), *via* the addition of one more chlorine substituent and changes within the ether linker, resulted in two the strongest 5-HT$_6$R agents (**4** and **9**), in 2-fold more active than **MST4,** the most potent triazine 5-HT$_6$R ligand described so far. Furthermore, the performed elimination of the chlorine-substituent from the lead **1** gave a potent and highly selective ligand (**2**), displaying selectivity for 5-HT$_6$R in the range of 71–867, with respect to 5-HT$_{2A}$, 5-HT$_7$ and D$_2$ dopamine receptors. SAR studies supported by crystallography and extended molecular modelling indicated that (i) the short linker branched with ethyl chain and (ii) the dichloro-substituted phenyl ring at positions *ortho* and *meta* are the most favorable structural factors for strong interaction with the target 5-HT$_6$R, but the role of the first one is predominant.

The performed study allows to find the new "hit', *i.e.* 4-[1-(2,5-dichlorophenoxy)propyl]-6-(4-methylpiperazin-1-yl)-1,3,5-triazin-2-amine (**9**), which displayed extremely high 5-HT$_6$R antagonistic action in the functional assays, significant procognitive effects *in vivo* in rats, very good permeability in PAMPA model and a satisfying safety *in vitro*. However, the disadvantageous weak metabolic stability of **9** and its methyl-branched analogue (**8**) was indicated *in vitro*, which requires a further pharmacomodulation.

Apart from compound **9**, its 2,3-dichlorophenyl analogue (**4**), found as the equally active 5-HT$_6$R agent, as well as the most selective phenyl-unsubstituted compound **2** seem to be worth of wider considerations, too. Thus, the presented results set the new lead structures for further studies concerning search for 5-HT$_6$R agents, which may be a useful tool for future treatment of cognitive impairment associated with Alzheimer Disease.

4. Experimental

4.1. Chemical synthesis

Melting points (mp) were determined using MEL-TEMP II apparatus and are uncorrected. ^{1}H NMR and ^{13}C NMR spectra were recorded on a Varian Mercury-VX 400 MHz PFG instrument or FT-NMR JEOL (JNM-ECZR500 RS1 v. ECZR) 500 MHz instrument (^{13}C NMR for **3**–**20**) in DMSO-d_6 (for almost all compounds, except from compound **2**–400 MHz) at ambient temperature using the solvent signal as an internal standard: the values of the chemical shifts expressed as δ values in (ppm) and the coupling constants (J) in Hz. Data are reported as follows: chemical shift, multiplicity (s, singlet; br. s, broad singlet; d, doublet; t, triplet; dd, doublet of doublet, q, quintet, m, multiplet), coupling constant J, number of protons,

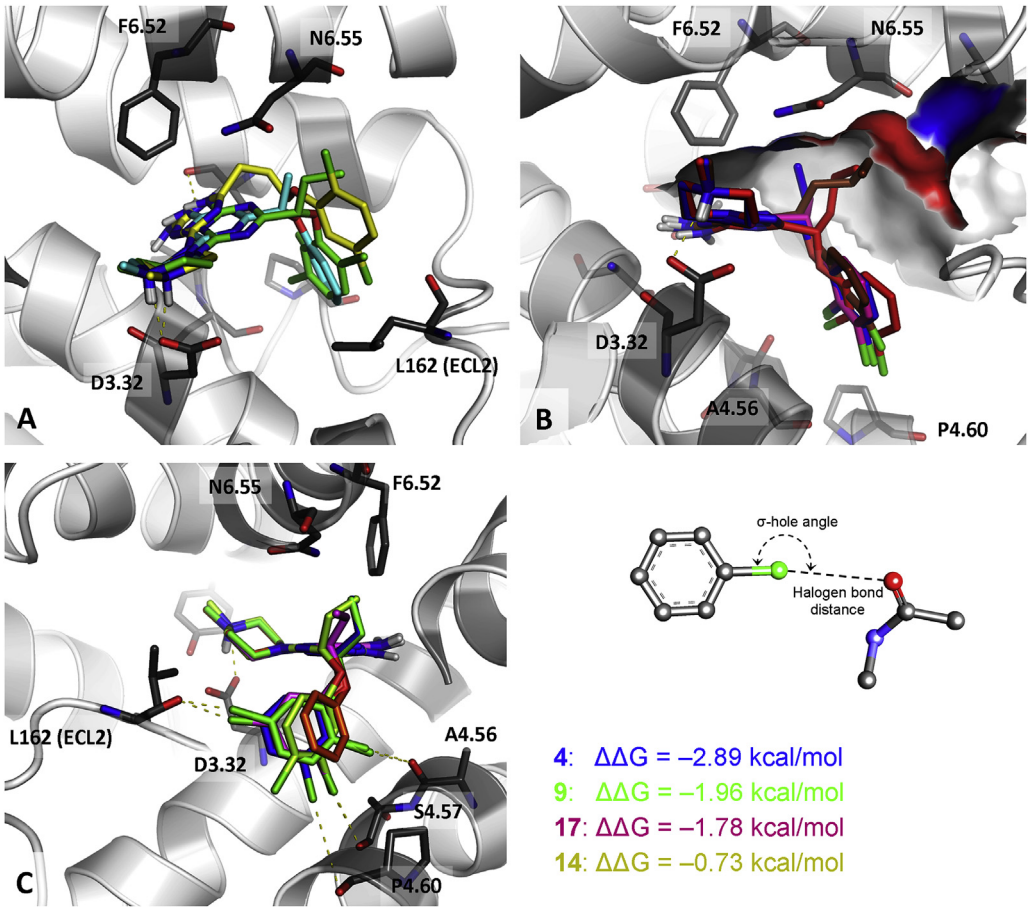

Fig. 9. Illustration of the binding modes of selected 1,3,5-triazine derivatives with 5-HT_6 receptor. (A) Comparison of the docking poses for compounds **9** (green), **12** (yellow), and the lead structure **1** (cyan). (B) Binding modes of analogues with methyl (**3**—pink), ethyl (**4**—blue), propyl (**5**—red), and butyl (**6**—brown) linker branch. (C) Comparison of the binding modes of unsubstituted **2** (orange) with its differently disubstituted of chlorine atoms derivatives, namely: 2,3-diCl (**4**—blue), 3,5-diCl (**17**—violet), 2,5-diCl (**9**—green), and 3,4-diCl (**14**—limon). Amino acids that are crucial for the binding of the presented compounds are shown as thick dark-grey sticks. (For interpretation of the references to color in this figure legend, the reader is referred to the Web version of this article.)

protons position (Pip-piperazine, Ph-phenyl). Mass spectra recorded on a UPLC—MS/MS system consisted of a Waters ACQUITY® UPLC® (Waters Corporation, Milford, MA, USA) coupled to a Waters TQD mass spectrometer (electrospray ionization mode ESI-tandem quadrupole). The UPLC/MS purity of all the final compounds was confirmed to be higher than 95% (except **14**). Retention time values (t_R) are given in minutes. Thin-layer chromatography (TLC) was performed on pre-coated Merck silica gel 60 F254 aluminum sheets (Hex/EtOAc 4:1, DCM/MeOH 95:5). The reactions at fixed temperature were carried out using a magnetic stirrer with a contact thermometer Heidolph MR 2001. Intermediates (**22**—**40**) were synthesized based on previous methods [28—31], and used in a crude form (purity 54—99%) for synthesis of the final compounds (**2**—**20**). Details of their synthesis and chemical characterization are provided in Supplementary.

*4.1.1. General procedure for the synthesis of final compounds (**2**—**20**)*

Sodium (10 mmol) was dissolved in 10 ml of absolute methanol, then 4-methylpiperazine-1-yl biguanide hydrochloride (**21**) (5 mmol) and a proper ester (**22**—**40**, 5 mmol) was added. The reaction mixture was refluxed for 15—30 h. After cooling to room temperature, the residue was washed with water (10 ml), stirred for 30 min at room temperature. The precipitated product was isolated by filtration and crystallized from methanol to give the desire final products as solids (method A). In case of lack of desirable precipitate, final product was converted into hydrochloric salt form using solution of HCl in diethyl ether (method B).

*4.1.1.1. (RS)-4-(4-methylpiperazin-1-yl)-6-(1-phenoxypropyl)-1,3,5-triazin-2-amine (**2**).* Ester **22**, reaction time: 16 h. Method A. White solid. Yield 38%, LC/MS^+ purity: 96,4%, t_R = 3.29, mp = 112—114 °C, $C_{17}H_{24}N_6O$ (MW = 328.42). ^{1}H NMR (400 MHz, DMSO-d_6) δ [ppm]: 0.97 (t, J = 7.4 Hz, 3H, CH_3), 1.84—1.93 (m, 2H, CH_2), 2.17 (s, 3H, N—CH_3), 2.27 (br. s, 4H, Pip-3,5-*H*), 3.66 (br. s, 4H, Pip-2,6-*H*), 4.63 (t, J = 6.5 Hz, 1H, O—CH), 6.77—6.89 (m, 4H, Ph-2,3,5,6-*H*), 7.00 (br. s, 1H, Ph-4-*H*), 7.18—7.24 (m, 2H, NH_2). ^{13}C NMR (101 MHz, DMSO-d_6) δ [ppm]: 10.50, 27.90, 42.86, 46.22, 54.70, 81.40, 115.56, 120.84, 129.78, 158.82, 164.94, 167.41, 176.51.

*4.1.1.2. (RS)-4-[1-(2,3-dichlorophenoxy)ethyl]-6-(4-methylpiperazin-1-yl)-1,3,5-triazin-2-amine (**3**).* Ester **23**, reaction time: 15 h. Method A. White solid. Yield 24%, LC/MS^+ purity: 100%, t_R = 4.15, mp = 187—189 °C, $C_{16}H_{20}Cl_2N_6O$ (MW = 383.28). ^{1}H NMR (500 MHz, DMSO-d_6) δ [ppm]: 1.54 (d, J = 5.73 Hz, 3H, CH_3) 2.13 (s, 3H, N—CH_3), 2.21 (br. s, 4H, Pip-3,5-H), 3.60 (br. s, 4H, Pip-2,6-H), 5.00 (d, J = 6.30 Hz, 1H, O—CH), 6.68—6.99 (m, 2H, NH_2), 6.87—6.89 (d def., 1H, Ph-6-*H*), 7.09—7.10 (m, 1H, Ph-5-*H*), 7.16 (t, J = 7.20 Hz, 1H, Ph-4-*H*). ^{13}C NMR (126 MHz, DMSO-d_6) δ [ppm]: 20.72, 43.02, 46.25, 54.72, 77.63, 113.86, 120.93, 122.40, 128.67, 132.83, 155.71,

164.90, 167.49, 176.25.

*4.1.1.3. (RS)-4-[1-(2,3-dichlorophenoxy)propyl]-6-(4-methylpiperazin-1-yl)-1,3,5-triazin-2-amine (**4**).* Ester **24**, reaction time: 21 h. Method A. White solid. Yield 40%, LC/MS$^+$ purity: 100%, t_R = 4.73, mp = 174–176 °C, $C_{17}H_{22}Cl_2N_6O$ (MW = 397.30). ^{1}H NMR (500 MHz, DMSO-d_6) δ [ppm]: 1.02 (t, J = 7.4 Hz, 3H, CH_3), 1.97 (p, J = 7.3 Hz, 2H, CH_2), 2.16 (s, 3H, N–CH_3), 2.25 (br. s, 4H, Pip-3,5-*H*), 3.63 (br. s, 4H, Pip-2,6-*H*), 4.80 (t, J = 6.3 Hz, 1H, O–CH), 6.86–6.89 (m, 1H, Ph-6-*H*), 7.01 (br. s, 2H, NH_2), 7.13–7.16 (m, 1H, Ph-5-*H*), 7.19–7.23 (m, 1H, Ph-4-*H*). ^{13}C NMR (126 MHz, DMSO-d_6) δ [ppm]: 10.38, 27.90, 46.26, 54.73, 82.57, 113.76, 120.91, 122.35, 128.75, 132.79, 155.93, 164.83, 167.41, 175.53.

*4.1.1.4. (RS)-4-[1-(2,3-dichlorophenoxy)butyl]-6-(4-methylpiperazin-1-yl)-1,3,5-triazin-2-amine (**5**).* Ester **25**, reaction time: 18 h. Method A. White solid. Yield 18%, LC/MS$^+$ purity: 100%, t_R = 5.20, mp = 186–188 °C, $C_{18}H_{24}Cl_2N_6O$ (MW = 411.33). ^{1}H NMR (500 MHz, DMSO-d_6) δ [ppm]: 0.89 (t, J = 6.8 Hz, 3H,CH_3), 1.36–1.57 (m, 2H, CH_2), 1.78–1.98 (m, 2H, CH_2), 2.12 (s, 3H, N–CH_3), 2.21 (s, 2H, Pip-3,5-*H*), 2.46 (s, 2H, Pip-3,5-*H*), 3.59 (s, 4H, Pip-2,6-*H*), 4.76–4.88 (m, 1H, O–CH), 6.77–6.91 (m, 2H, NH_2), 6.98 (br. s, 1H, Ph-5-*H*), 7.07–7.23 (m, 2H, Ph-4,6-*H*). ^{13}C NMR (126 MHz, DMSO-d_6) δ [ppm]: 14.23, 18.81, 36.69, 46.26, 54.71, 81.17, 113.67, 120.86, 122.35, 128.76, 132.80, 155.91, 164.83, 167.41, 175.75.

*4.1.1.5. (RS)-4-[1-(2,3-dichlorophenoxy)penthyl]-6-(4-methylpiperazin-1-yl)-1,3,5-triazin-2-amine (**6**).* Ester **26**, reaction time: 19 h. Method A. White solid. Yield 52%, LC/MS$^+$ purity: 98,5%, t_R = 5.41, mp = 150–152 °C, $C_{19}H_{26}Cl_2N_6O$ (MW = 425.36). ^{1}H NMR (500 MHz, DMSO-d_6) δ [ppm]: 0.81 (t, J = 7.16 Hz, 3H, CH_3), 1.26–1.31 (q def., 2H, CH_2), 1.37–1.48 (m, 2H, CH_2), 1.85–1.95 (m, 2H, CH_2), 2.11 (s, 3H, N–CH_3) 2.20 (s, 4H, Pip-3,5-*H*), 3.31 (s, 4H, Pip-2,6-*H*), 4.78–4.81 (d def., 1H, O–CH), 6.82 (d, J = 7.45 Hz, 1H, Ph-6-*H*), 6.99–7.01 (m, 2H, NH_2), 7.09–7.10 (m, 1H, Ph-5-*H*), 7.14–7.15 (m, 1H, Ph-4-*H*). ^{13}C NMR (126 MHz, DMSO-d_6) δ [ppm]: 14.42, 22.40, 27.68, 34.30, 43.20, 46.26, 54.72, 81.45, 113.68, 120.89, 122.35, 128.74, 132.81, 155.92, 164.84, 167.42, 175.73.

*4.1.1.6. 4-[3-(2,3-dichlorophenoxy)propyl]-6-(4-methylpiperazin-1-yl)-1,3,5-triazin-2-amine (**7**).* Ester **27**, reaction time: 20 h. Method A. White solid. Yield 42%, LC/MS$^+$ purity: 100%, t_R = 4.18, mp = 84–86 °C, $C_{17}H_{22}Cl_2N_6O$ (MW = 397.30). ^{1}H NMR (500 MHz, DMSO-d_6) δ [ppm]: 2.08 (d, J = 6.30 Hz, 2H, CH_2), 2.12 (br. s, 3H, N–CH_3), 2.21 (br. s, 4H, Pip-3,5-*H*), 2.53 (t, J = 6.59 Hz, 2H, CH_2), 3.61 (br. s, 4H, Pip-2,6-*H*), 4.09 (br. s, 2H, O–CH_2), 6.74 (br. s, 2H, NH_2), 7.05 (d, J = 8.02 Hz, 1H, Ph-4-*H*), 7.14 (d, J = 8.02 Hz, 1H, Ph-6-*H*), 7.23 (t, J = 7.73 Hz, 1H, Ph-5-*H*). ^{13}C NMR (126 MHz, DMSO-d_6) δ [ppm]: 26.58, 34.89, 42.85, 46.30, 54.85, 69.24, 112.69, 120.61, 122.34, 128.98, 132.77, 155.99, 164.96, 167.30, 177.16.

*4.1.1.7. (RS)-4-[1-(2,5-dichlorophenoxy)ethyl]-6-(4-methylpiperazin-1-yl)-1,3,5-triazin-2-amine (**8**).* Ester **28**, reaction time: 22 h. Method A. White solid. Yield 43%, LC/MS$^+$ purity: 96,4%, t_R = 4.02, mp = 153–155 °C, $C_{16}H_{20}Cl_2N_6O$ (MW = 383.28). ^{1}H NMR (500 MHz, DMSO-d_6) δ [ppm]: 1.53 (d, J = 6.87 Hz, 3H, CH_3), 2.12 (s, 3H, N–CH_3), 2.21 (br. s, 4H, Pip-3,5-*H*), 3.61 (br. s, 4H, Pip-2,6-*H*), 5.01 (q, J = 6.68 Hz, 1H, O–CH), 6.70–6.94 (m., 2H, NH_2) 6.92–6.94 (d def., 1H, Ph-4-*H*), 7.06 (s, 1H, Ph-6-H), 7.37 (d, J = 8.02 Hz, 1H, Ph-3-*H*). ^{13}C NMR (126 MHz, DMSO-d_6) δ [ppm]: 20.43, 43.09, 46.25, 54.75, 77.65, 115.77, 121.05, 121.74, 131.46, 132.38, 154.76, 164.82, 167.53, 175.91.

*4.1.1.8. (RS)-4-[1-(2,5-dichlorophenoxy)propyl]-6-(4-methylpiperazin-1-yl)-1,3,5-triazin-2-amine (**9**).* Ester **29**, reaction time: 20 h. Method A. White solid. Yield 47%, LC/MS$^+$ purity: 100%, t_R = 4.60, mp = 163–165 °C, $C_{17}H_{22}Cl_2N_6O$ (MW = 397.30). ^{1}H NMR (500 MHz, DMSO-d_6) δ [ppm]: 0.94 (t, J = 7.45 Hz, 3H, CH3), 1.91 (q, J = 7.16 Hz, 2H, CH_2), 2.11 (s, 3H, N–CH_3), 2.21 (br. s, 4H, Pip-3,5-*H*), 3.61 (br. s, 4H, Pip-2,6-*H*), 4.77 (t, J = 6.30 Hz, 1H, O–CH), 6.84–6.90 (m, 2H, NH_2), 6.90–6.93 (d def., 1H, Ph-6-*H*), 7.02–7.05 (d def., 1H, Ph-4-*H*), 7.36 (d, J = 8.59 Hz, 1H, Ph-3-*H*). ^{13}C NMR (126 MHz, DMSO-d_6) δ [ppm]: 10.25, 27.60, 43.11, 46.23, 54.74, 82.69, 115.66, 121.11, 121.66, 131.41, 132.39, 155.01, 164.79, 167.49, 175.23.

*4.1.1.9. (RS)-4-[1-(2,5-dichlorophenoxy)butyl]-6-(4-methylpiperazin-1-yl)-1,3,5-triazin-2-amine (**10**).* Ester **30**, reaction time: 22 h. Method A. White solid. Yield 54%, LC/MS$^+$ purity: 96,7%, t_R = 5.13, mp = 143–145 °C, $C_{18}H_{24}Cl_2N_6O$ (MW = 411.33). ^{1}H NMR (500 MHz, DMSO-d_6) δ [ppm]: 0.92 (t, J = 7.4 Hz, 3H, CH_3), 1.37–1.55 (m, 2H, CH_2), 1.83–2.00 (m, 2H, CH_2), 2.16 (s, 3H, N–CH_3), 2.25 (br. s, 4H, Pip-3,5-*H*), 3.57–3.74 (m, 4H, Pip-2,6-*H*), 4.88 (dd, J_1 = 8.2 Hz, J_2 = 4.9 Hz, 1H, O–CH), 6.90–6.94 (m, 1H, NH_2), 6.96–6.98 (m, 1H, Ph-6-*H*), 7.05 (d, J = 2.3 Hz, 1H, Ph-4-*H*), 7.06–7.09 (m, 1H, NH_2), 7.41–7.44 (m, 1H, Ph-3-*H*). ^{13}C NMR (126 MHz, DMSO-d_6) δ [ppm]: 175.43, 167.46, 164.77, 154.97, 132.37, 131.47, 121.70, 121.05, 115.60, 81.24, 54.74, 46.27, 36.38, 18.70, 14.25.

*4.1.1.10. (RS)-4-[1-(2,5-dichlorophenoxy)penthyl]-6-(4-methylpiperazin-1-yl)-1,3,5-triazin-2-amine (**11**).* Ester **31**, reaction time: 25 h. Method A. White solid. Yield 33%, LC/MS$^+$ purity: 98,8%, t_R = 5.34, mp = 143–145 °C, $C_{19}H_{26}Cl_2N_6O$ (MW = 425.36). ^{1}H NMR (500 MHz, DMSO-d_6) δ [ppm]: 0.80 (t, J = 7.16 Hz, 3H, CH_3), 1.24–1.32 (m, 2H, CH_2), 1.35–148 (m, 2H, CH_2), 1.85–1.96 (m, 2H, CH_2), 2.11 (s, 3H, N–CH_3), 2.20 (br. s, 4H, Pip-3,5-*H*), 3.61 (br. s, 4H, Pip-2,6-*H*), 4.80–4.83 (m, 1H, O–CH), 6.84–6.92 (m, 2H, NH_2), 6.90–6.92 (m, 1H, Ph-6-*H*), 7.01 (d, J = 2.29 Hz, 1H, Ph-4-*H*), 7.36 (d, J = 8.02 Hz, 1H, Ph-3-*H*). ^{13}C NMR (126 MHz, DMSO-d_6) δ [ppm]: 14.39, 22.42, 27.58, 34.02, 43.02, 46.23, 54.75, 81.56, 115.60, 121.08, 121.65, 131.41, 132.40, 154.98, 164.79, 167.50, 175.41.

*4.1.1.11. 4-[3-(2,5-dichlorophenoxy)propyl]-6-(4-methylopiperazin-1-yl)-1,3,5-triazin-2-amine (**12**).* Ester **32**, reaction time: 16 h. Method A. White solid. Yield 28%, LC/MS$^+$ purity: 98,8%, t_R = 3.71, mp = 126–128 °C, $C_{17}H_{22}Cl_2N_6O$ (MW = 397.30). ^{1}H NMR (500 MHz, DMSO-d_6) δ [ppm]: 2.05–2.06 (m, 2H, CH_2), 2.12 (br. s, 3H, N–CH_3), 2.21 (br. s, 4H, Pip-3,5-*H*), 2.50 (t, J = 7.16 Hz, 2H, CH_2), 3.62 (br. s, 4H, Pip-2,6-*H*), 4.09 (t, J = 6.01 Hz, 2H, O–CH_2), 6.70 (br. s, 2H, NH_2), 6.94–6.96 (m, 1H, Ph-4-*H*), 7.16 (s, 1H, Ph-6-*H*), 7.37 (d, J = 8.59 Hz, 1H, Ph-3-*H*). ^{13}C NMR (126 MHz, DMSO-d_6) δ [ppm]: 26.56, 34.81, 42.87, 46.31, 54.86, 69.14, 114.50, 120.80, 121.58, 131.32, 132.94, 155.14, 164.97, 167.30, 177.14.

*4.1.1.12. (RS)-4-[1-(3,4-dichlorophenoxy)ethyl]-6-(4-methylopiperazin-1-yl)-1,3,5-triazin-2-amine hydrochloride (**13**).* Ester **33**, reaction time: 30 h. Method B. White solid. Yield 13%, LC/MS$^+$ purity: 100%, t_R = 4.28, mp = 258–260 °C, $C_{16}H_{20}Cl_2N_6O$ (MW = 383.11). ^{1}H NMR (500 MHz, DMSO-d_6) δ [ppm]: 1.55 (d, J = 6.87 Hz, 3H, CH_3), 2.70 (br. s, 3H, N–CH_3), 3.03 (br. s, 4H, Pip-3,5-*H*), 4.55–4.63 (m, 4H, Pip-2,6-*H*), 5.31 (d, J = 6.30 Hz, 1H, O–CH), 7.06–7.08 (m, 1H, Ph-6-*H*), 7.38–7.39 (m, 1H, Ph-2-*H*), 7.48–7.49 (m, 1H, Ph-5-*H*), 8.18–8.36 (m, 2H, NH_2), 11.85 (br. s, 1H, NH^+). ^{13}C NMR (126 MHz, DMSO-d_6) δ [ppm]: 19.67, 42.44, 51.69, 51.91, 74.69, 116.98, 118.55, 123.87, 131.49, 132.01, 156.82, 162.80.

*4.1.1.13. (RS)-4-[1-(3,4-dichlorophenoxy)propyl]-6-(4-methylopiperazin-1-yl)-1,3,5-triazin-2-amine (**14**).* Ester **34**, reaction time: 20 h. Method A. White solid. Yield 50%, LC/MS$^+$ purity: 91,4%, t_R = 4.61, mp = 126–128 °C, $C_{17}H_{22}Cl_2N_6O$ (MW = 397.30). ^{1}H NMR (500 MHz, DMSO-d_6) δ [ppm]: 0.90 (t, J = 7.45 Hz, 3H, CH_3),

1.84 (q, $J = 6.70$ Hz, 2H, CH_2), 2.11 (s, 3H, N—CH_3), 2.21 (br. s, 4H, Pip-3,5-*H*), 3.61 (br. s, 4H, Pip-2,6-*H*), 4.67 (t, $J = 6.30$ Hz, 1H, O—CH), 6.82—6.84 (m, 1H, Ph-6-*H*), 6.82—7.00 (m, 2H, NH_2), 7.12 (s, 1H, Ph-2-*H*), 7.40 (d, $J = 9.16$ Hz, 1H, Ph-3-*H*). ^{13}C NMR (126 MHz, DMSO-d_6) δ [ppm]: 10.34, 27.64, 43.11, 46.26, 54.73, 81.99, 116.52, 117.74, 122.80, 131.36, 131.81, 158.35, 164.85, 167.42, 175.57.

*4.1.1.14. 4-[3-(3,4-dichlorophenoxy)propyl]-6-(4-methylopiperazin-1-yl)-1,3,5-triazin-2-amine (**15**).* Ester **35**, reaction time: 18 h. Method A. White solid. Yield 45%, LC/MS$^+$ purity: 99,2%, $t_R = 3.91$, mp = 90—92 °C, $C_{17}H_{22}Cl_2N_6O$ (MW = 397.30). ^{1}H NMR (500 MHz, DMSO-d_6) δ [ppm]: 2.01—2.03 (m, 2H, CH_2), 2.12 (s, 3H, N—CH_3), 2.20 (br. s, 4H, Pip-3,5-*H*), 2.46—2.47 (m, 2H, CH_2), 3.61 (br. s, 4H, Pip-2,6-*H*), 3.98 (t, $J = 6.01$ Hz, 2H, O—CH_2), 6.74 (br. s, 2H, NH_2), 6.86—6.89 (m, 1H, Ph-6-H), 7.12 (d, $J = 2.29$ Hz, 1H, Ph-2-H), 7.42 (d, $J = 9.16$ Hz, 1H, Ph-3-*H*). ^{13}C NMR (126 MHz, DMSO-d_6) δ [ppm]: 26.60, 34.85, 42.85, 46.29, 54.84, 68.40, 115.89, 116.80, 122.72, 131.40, 132.09, 158.62, 164.94, 167.29, 177.19.

*4.1.1.15. (RS)-4-[1-(3,5-dichlorophenoxy)ethyl]-6-(4-methylopiperazin-1-yl)-1,3,5-triazin-2-amine (**16**).* Ester **36**, reaction time: 20 h. Method A. White solid. Yield 29%, LC/MS$^+$ purity: 100%, $t_R = 4.33$, mp = 180—182 °C, $C_{16}H_{20}Cl_2N_6O$ (MW = 383.28). ^{1}H NMR (500 MHz, DMSO-d_6) δ [ppm]: 1.48 (d, $J = 6.30$ Hz, 3H, CH_3), 2.12 (s, 3H, N—CH_3), 2.21 (s, 4H, Pip-3,5-*H*), 3.31 (s, 4H, Pip-2,6-*H*), 4.96 (q, $J = 6.30$ Hz, 1H, O—CH), 6.88 (br. s, 2H, NH_2), 6.93 (d, $J = 1.72$ Hz, 2H, Ph-2,6-*H*), 7.03 (s, 1H, Ph-4-*H*). ^{13}C NMR (126 MHz, DMSO-d_6) δ [ppm]: 20.40, 42.90, 46.25, 54.74, 77.03, 115.13, 120.74, 134.86, 160.00, 164.86, 167.50, 176.09.

*4.1.1.16. (RS)-4-[1-(3,5-dichlorophenoxy)propyl]-6-(4-methylpiperazin-1-yl)-1,3,5-triazin-2-amine (**17**).* Ester **37**, reaction time: 16 h. Method A. White solid. Yield 48%, LC/MS$^+$ purity: 100%, $t_R = 4.90$, mp = 124—126 °C, $C_{17}H_{22}Cl_2N_6O$ (MW = 397.30). ^{1}H NMR (500 MHz, DMSO-d_6) δ [ppm]: 0.95 (t, $J = 7.4$ Hz, 3H, CH_3), 1.88—1.95 (m, 2H, CH_2), 2.16 (s, 3H, N—CH_3), 2.25 (br. s, 4H, Pip-3,5-*H*), 3.54—3.76 (br. s, 4H, Pip-2,6-*H*), 4.77 (t, $J = 6.5$ Hz, 1H, O—CH), 6.91 (br. s, 1H, NH_2), 6.97 (d, $J = 1.8$ Hz, 2H, Ph-2,6-*H*), 7.03 (br. s, 1H, NH_2), 7.10 (t, $J = 1.8$ Hz, 1H, Ph-4-*H*). ^{13}C NMR (126 MHz, DMSO-d_6) δ [ppm]: 10.29, 27.48, 46.27, 54.76, 82.09, 115.16, 120.74, 134.85, 160.33, 164.81, 167.42, 175.35.

*4.1.1.17. (RS)-4-[1-(3,5-dichlorophenoxy)butyl]-6-(4-methylpiperazin-1-yl)-1,3,5-triazin-2-amine (**18**).* Ester **38**, reaction time: 21 h. Method A. White solid. Yield 46%, LC/MS$^+$ purity: 98,3%, $t_R = 5.26$, mp = 164—166 °C, $C_{18}H_{24}Cl_2N_6O$ (MW = 411.33). ^{1}H NMR (500 MHz, DMSO-d_6) δ [ppm]: 0.90 (t, $J = 7.3$ Hz, 3H, CH_3), 1.31—1.49 (m, 2H, CH_2), 1.79—1.91 (m, 2H, CH_2), 2.16 (s, 3H, N—CH_3), 2.25 (br. s, 4H, Pip-3,5-*H*), 3.63 (br. s, 4H, Pip-2,6-*H*), 4.83 (dd, $J_1 = 7.8$ Hz, $J_2 = 5.2$ Hz, 1H, O—CH), 6.91 (br. s, 1H, NH_2), 6.94—6.97 (m, 2H, Ph-2,6-*H*), 7.03 (br. s, 1H, NH_2), 7.07—7.10 (m, 1H, Ph-4-*H*). ^{13}C NMR (126 MHz, DMSO-d_6) δ [ppm]: 175.57, 167.42, 164.81, 160.30, 134.86, 120.75, 115.12, 80.65, 54.73, 46.26, 36.34, 18.72, 14.21.

*4.1.1.18. (RS)-4-[1-(3,5-dichlorophenoxy)pentyl]-6-(4-methylpiperazin-1-yl)-1,3,5-triazin-2-amine (**19**).* Ester: **39**, reaction time: 22 h. Method A. White solid. Yield 44%, LC/MS$^+$ purity: 99,5%, $t_R = 5.70$, mp = 154—156 °C, $C_{19}H_{26}Cl_2N_6O$ (MW = 425.36). ^{1}H NMR (500 MHz, DMSO-d_6) δ [ppm]: 0.86 (t, $J = 5.4$ Hz, 3H, CH_3), 1.25—1.46 (m, 4H, CH_2—CH_2), 1.84—1.93 (m, 2H, CH_2), 2.16 (s, 3H, N—CH_3), 2.25 (s, 4H, Pip-3,5-*H*), 3.64 (s, 4H, Pip-2,6-*H*), 4.79—4.84 (m, 1H, O—CH), 6.91 (br. s, 1H, NH_2), 6.95—6.98 (m, 2H, Ph-2,6-*H*), 7.04 (br. s, 1H, NH_2), 7.08—7.11 (m, 1H, Ph-4-*H*). ^{13}C NMR (126 MHz, DMSO-d_6) δ [ppm]: 14.40, 22.42, 27.55, 33.98, 46.21, 54.74, 80.90, 115.12, 120.75, 134.86, 160.29, 164.80, 167.43, 175.55.

*4.1.1.19. 4-[3-(2,4-dichlorophenoxy)propyl]-6-(4-methylpiperazin-1-yl)-1,3,5-triazin-2-amine (**20**).* Ester **40**, reaction time: 17 h. Method A. White solid. Yield 43%, LC/MS$^+$ purity: 100%, t_R = 4.09, mp = 150—152 °C, $C_{17}H_{22}Cl_2N_6O$ (MW = 397.30). ^{1}H NMR (500 MHz, DMSO-d_6) δ [ppm]: 2.06—2.07 (m, 2H, CH_2), 2.12 (br. s, 3H, N—CH_3), 2.21 (br. s, 4H, Pip-3,5-*H*), 2.52 (br. s, 2H, CH_2), 3.62 (br. s, 4H, Pip-2,6-*H*), 4.06 (br. s, 2H, O—CH_2), 6.73 (br. s, 2H, NH_2), 7.10 (br. s, 1H, Ph-6-*H*), 7.29 (br. s, 1H, Ph-5-*H*), 7.49 (br. s, 1H, Ph-3-*H*). ^{13}C NMR (126 MHz, DMSO-d_6) δ [ppm]: 26.56, 34.84, 42.85, 46.30, 54.86, 69.04, 115.46, 122.91, 124.75, 128.58, 129.73, 153.57, 164.97, 167.30, 177.15.

4.2. X-ray crystallographic studies

Crystals suitable for an X-ray structure analysis for both compounds were obtained from methanol by slow evaporation of the solvent at room temperature.

Data for single crystals were collected using the XtaLAB Synergy-S diffractometer, equipped with the Cu (1.54184 Å) Kα radiation source and graphite monochromator. The phase problem was solved by direct methods using SIR-2014 [48] and all non-hydrogen atoms were refined anisotropically using weighted full-matrix least-squares on F^2. Refinement and further calculations were carried out using SHELXL [49]. The hydrogen atoms bonded to carbons were included in the structure at idealized positions and were refined using a riding model with U_{iso}(H) fixed at 1.5 U_{eq}(C) for methyl groups and 1.2 U_{eq}(C) for the other hydrogen atoms. Hydrogen atoms attached to nitrogen atoms were found from the difference Fourier map and refined without any restraints. For molecular graphics MERCURY [50] program was used.

Crystallographic data for 9: $C_{17}H_{22}Cl_2N_6O$, M_r = 397.30, wavelength 1.54184 Å, crystal size = 0.13 × 0.18 × 0.60 mm^3, triclinic, space group P$\bar{1}$, a = 8.6624(3) Å, b = 9.8661(4) Å, c = 12.2609(5) Å, α = 70.529(4)°, β = 77.394(3)°, γ = 86.601(3)°, V = 964.02(7) Å^3, Z = 2, T = 100(2) K, 25842 reflections collected, 3867 unique reflections (R_{int} = 0.0301), R1 = 0.0314, w*R*2 = 0.0777 [I > 2σ(I)], R1 = 0.0325, w*R*2 = 0.0786 [all data].

Crystallographic data for 20: $C_{17}H_{22}Cl_2N_6O$, M_r = 397.30, wavelength 1.54184 Å, crystal size = 0.08 × 0.15 × 0.39 mm^3, monoclinic, space group $P2_1/n$, a = 15.5045(1) Å, b = 6.4311(1) Å, c = 18.8146(5) Å, β = 94.185(1)°, V = 1871.02(3) Å^3, Z = 4, T = 100(2) K, 56835 reflections collected, 3876 unique reflections (R_{int} = 0.0391), R1 = 0.0276, w*R*2 = 0.0727 [I > 2σ(I)], R1 = 0.0285, w*R*2 = 0.0733 [all data].

CCDC 1980289 and 1980290 contain the supplementary crystallographic data. These data can be obtained free of charge from The Cambridge Crystallographic Data Centre *via* www.ccdc.cam.ac.uk/data_request/cif.

4.3. Molecular modelling

4.3.1. Molecular docking

The procedure of 5-HT_6R homology models generation (β_2 adrenergic receptor template), its use for analysis of the binding mode of our other 1,3,5-triazine derivatives (to support structure-activity relationship analyses) was described previously [31]. In order to select the relevant subset of the 5-HT_6 receptor conformations, the newly synthesized compounds (**2**—**20**) were docked and analyzed. Only models showing coherent binding mode to the previously described 1,3,5-triazine derivatives, and explaining the main structure-activity relationships were used.

The three-dimensional structures of the synthesized compounds were prepared using LigPrep [51], and the appropriate ionization states at pH 7.4 ± 1.0 were assigned using Epik [52]. Protein Preparation Wizard was used to assign the bond orders,

check for steric clashes and assign appropriate amino acid ionization states for each receptor model. The receptor grids were generated (OPLS3 force field [53]) by centering the grid box with a size of 12 Å on the D3.32 residue. Docking was performed by quantum-polarized ligand docking (QPLD) procedure [54] involves the QM-derived ligand atomic charges in the protein environment at the B3PW91/ccpVTZ level. Only the best ten poses per ligand returned by the procedure were considered.

4.3.2. Binding free energy calculations

MM/GBSA (Generalized-Born/Surface Area) was used to calculate the binding free energy based on the ligand−receptor complexes generated by the QPLD procedure. The ligand poses were minimized using the local optimization feature in Prime, the flexible residue distance was set to 6.0 Å from a ligand pose, and the ligand charges obtained in the QPLD stage were used. The energies of complexes were calculated with the OPLS3e force field and Generalized-Born/Surface Area continuum solvent model. To assess the influence of a given substituent on the binding, the ΔΔG was calculated as a difference between binding free energy (ΔG) of unsubstituted at phenyl ring and dichlorinated analogues.

4.4. Evaluation of 5-HT_6R, 5-HT_{2A}R, 5-HT_7R, D_2R affinities

4.4.1. Cell culture and preparation of cell membranes for radioligand binding assays

HEK293 cells with stable expression of human 5-HT_6, 5-HT_{7b} and D_{2L} receptors (prepared with the use of Lipofectamine 2000) or CHO−K1 cells with plasmid containing the sequence coding for the human serotonin 5-HT_{2A} receptor (Perkin Elmer) were maintained at 37 °C in a humidified atmosphere with 5% CO_2 and grown in Dulbecco's Modifier Eagle Medium containing 10% dialyzed fetal bovine serum and 500 μg/ml G418 sulfate. For membrane preparation, cells were subcultured in 150 cm^2 flasks, grown to 90% confluence, washed twice with prewarmed to 37 °C phosphate buffered saline (PBS) and pelleted by centrifugation (200×*g*) in PBS containing 0.1 mM EDTA and 1 mM dithiothreitol. Prior to membrane preparation, pellets were stored at −80 °C.

4.4.2. Radioligand binding assays

Cell pellets were thawed and homogenized in 10 vol of assay buffer using an Ultra Turrax tissue homogenizer and centrifuged twice at 35,000 g for 15 min at 4 °C, with incubation for 15 min at 37 °C in between. The composition of the assay buffers was as follows: for 5-HT_{2A}R: 50 mM Tris HCl, 0.1 mM EDTA, 4 mM $MgCl_2$ and 0.1% ascorbate; for 5-HT_6R: 50 mM Tris HCl, 0.5 mM EDTA and 4 mM $MgCl_2$, for 5- HT_{7b}R: 50 mM Tris HCl, 4 mM $MgCl_2$, 10 μM pargyline and 0.1% ascorbate; for dopamine D_{2L}R: 50 mM Tris HCl, 1 mM EDTA, 4 mM $MgCl_2$, 120 mM NaCl, 5 mM KCl, 1.5 mM $CaCl_2$ and 0.1% ascorbate. All assays were incubated in a total volume of 200 μL in 96-well microtitre plates for 1 h at 37 °C, except 5-HT_{2A}R which were incubated at 27 °C. The process of equilibration was terminated by rapid filtration through Unifilter plates with a 96-well cell harvester and radioactivity retained on the filters was quantified on a Microbeta plate reader (PerkinElmer, USA). For displacement studies the assay samples contained as radioligands (PerkinElmer, USA): 1 nM [^{3}H]-ketanserin (53.4 Ci/mmol) for 5-HT_{2A}R; 2 nM [^{3}H]-LSD (83.6 Ci/mmol) for 5-HT_6R; 0.8 nM [^{3}H]-5-CT (39.2 Ci/mmol) for 5-HT_7R or 2.5 nM [^{3}H]-raclopride (76.0 Ci/mmol) for D_{2L}R. Non-specific binding was defined with 10 μM of 5-HT in 5-HT_7R binding experiments, whereas 20 μM of mianserin, 10 μM of methiothepine or 10 μM of haloperidol were used in 5-HT_{2A}R, 5-HT_6R and D_{2L} assays, respectively. Each compound was tested in triplicate at 7 concentrations (10^{-10}-10^{-4} M). The inhibition constants (K_i) were calculated from the Cheng-Prusoff equation [55]. Results were expressed as means of at least two separate experiments.

4.5. Functional assays for 5-HT_6 receptor

Test and reference compounds were dissolved in dimethyl sulfoxide (DMSO) at a concentration of 10 mM. Serial dilutions were prepared in 96-well microplate in assay buffer and 8 to 10 concentrations were tested. For the 5-HT_6, adenylyl cyclase activity were monitored using cryopreserved 1321N1 cells with expression of the human serotonin 5-HT_6 receptor (Perkin Elmer, USA). Thawed cells were resuspended in stimulation buffer (HBSS, 5 mM HEPES, 0.5 IBMX, and 0.1% BSA at pH 7.4) at 3×10^5 cells/ml. The same volume (10 μl) of cell suspension was added to tested compounds. Samples were loaded onto a white opaque half area 96-well microplate. The antagonist response experiment was performed with 22 nM serotonin as the reference agonist for 5-HT_6 receptor. The agonist and antagonist were added simultaneously. Cell stimulation was performed for 30 min at room temperature. After incubation, cAMP measurements were performed with homogeneous TR-FRET immunoassay using the LANCE Ultra cAMP kit (PerkinElmer, USA). 10 μl of EucAMP Tracer Working Solution and 10 μl of ULight-anti-cAMP Tracer Working Solution were added, mixed, and incubated for 1 h. The TR-FRET signal was read on an EnVision microplate reader (PerkinElmer, USA). IC 50 and EC 50 were determined by nonlinear regression analysis using GraphPad Prism 7.0 software.

4.6. Drug-likeness

4.6.1. References

The following references used in ADMETox studies *in vitro*: caffeine (CFN), carbonyl cyanide 3-chlorophenylhydrazone, (CCCP) and doxorubicin (DX) were provided by Sigma-Aldrich (St. Louis, MO, USA).

4.6.2. Permeability

Pre-coated PAMPA Plate System Gentest™ was used for estimation of compounds passive transport through cell membranes and was provided by Corning (Tewksbury, MA, USA). The assay was performed in accordance to the manufacturer recommendations and was previously described by our research group [32,34–38]. The concentrations in apical and basolateral wells were estimated using the LC/MS method with an internal standard. The permeability coefficient Pe was calculated according to the formulas described in the literature [33] and compared to the high permeable reference CFN.

4.6.3. Metabolic stability

The *in vitro* evaluation of metabolic pathways was performed by 120 min incubation of compounds with rat liver microsomes (RLMs) at 37 °C according the described previously procedures [32,34,35,37,38]. RLMs were provided by (Sigma-Aldrich, St. Louis, MO, USA). The LC/MS analyses were performed to determine the most probable structures of 5-HT_6R ligands' metabolites.

The *in silico* prediction of the most probable sites of metabolism was performed by MetaSite 6.0.1. Software provided by Molecular Discovery Ltd (Hertfordshire, UK).

4.6.4. Toxicity

Hepatoma HepG2 (ATCC® HB-8065™) cells were used for hepatotoxicity assessment. All assays and growth conditions were applied as we described before [37–40]. Tested compounds were added to the cells and incubated for 72 h in the four concentrations: 1, 10, 50 and 100 ĕM. The reference toxins CCCP and DX were added

at 10 μM and 1 μM, respectively. The cells' viability was determined by CellTiter 96® AQueous Non-Radioactive Cell Proliferation Assay (MTS) provided by Promega (Madison, WI, USA). The absorbance was measured using a microplate reader EnSpire (PerkinElmer, Waltham, MA USA) at 490 nm.

4.7. In vivo studies

4.7.1. Animals

The experiments were performed on male Wistar rats (230–260 g) obtained from an accredited animal facility at the Jagiellonian University Medical College, Poland. The animals were housed in group of four in controlled environment (ambient temperature 21 ± 2 °C; relative humidity 50–60%; 12-h light/dark cycles (lights on at 8:00). Standard laboratory food (LSM-B) and filtered water were freely available. Animals were assigned randomly to treatment groups. All the experiments were performed by two observers unaware of the treatment applied between 9:00 and 14:00 on separate groups of animals. All animals were used only once. Procedures involving animals and their care were conducted in accordance with current European Community and Polish legislation on animal experimentation. Additionally, all efforts were made to minimize animal suffering and to use only the number of animals necessary to produce reliable scientific data. The experimental protocols and procedures described in this manuscript were approved by the I Local Ethics Commission in Cracow (no 309/2019) and complied with the European Communities Council Directive of 24 November 1986 (86/609/EEC) and were in accordance with the 1996 NIH Guide for the Care and Use of Laboratory Animals.

4.7.2. Drugs

All compounds were suspended in 1% Tween 80 immediately before administration in a volume of 2 ml/kg. Compounds were administered intraperitoneally (*i.p.*) 60 min while MK-801 was given *i.p.* 30 min before testing. Control animals received vehicle (1% Tween 80) according to the same schedule.

4.7.3. Behavioral procedures in rats

4.7.3.1. Novel object recognition (NOR) test and Novel Object Location (NOL) test. Five days before the experiment, the rats were transferred to the laboratory, labeled and, thereafter, left to acclimate to the new environment. The animals were handling every five days before experiments to minimize the stress reaction. The protocol was adapted from the original work [56,57]. The test session comprising of two trials separated by an inter-trial interval (ITI) of 1 h was carried out on after two day of training session.

During the first trial (familiarization, T1) two identical objects (A1 and A2) were presented in the opposite corners of the open field, approximately 10 cm from the walls.

In the NOR test procedure:

During the second trial (recognition, T2) one of the A objects was replaced by a novel object B, so that the animals were presented with the A = familiar and B = novel objects. Both trials lasted for 3 min and the animals were returned to their home cages after T1.

In the NOL test procedure:

During the second trial (recognition, T2) one of the A objects was replaced to another place B, so that the animals were presented with the A = familiar location and B = novel location of objects. Both trials lasted for 3 min and the animals were returned to their home cages after T1.

The objects used were the metal Coca-Cola cans and the glass jars filled with the sand. The heights of the objects were comparable (~12 cm) and the objects were heavy enough not to be displaced by the animals. The sequence of presentations and the location of the objects was randomly assigned to each rat. After each measurement, the floor was cleaned and dried.

The animals explored the objects by looking, licking, sniffing or touching the object but not when leaning against, standing or sitting on the object. Any rat exploring the two objects for less than 5 s within 3 min of T1 or T2 was eliminated from the study. Exploration time of the objects was measured by blind experimenter. Based on exploration time (E) of two objects during T2, discrimination index (DI) was calculated according to the formula: DI = (EB−EA)/(EA + AB). Using this metric, scores approaching zero reflects no preference while positive values reflect preference for the novel object (or novel location of object) and negative numbers reflect preference for the familiar.

MK-801, used to attenuate learning, was administered at the dose of 0.1 mg/kg (*i.p.*) 30 min before familiarization phase (T1), while investigated compounds were given 60 min before T1 session.

4.7.4. Statistical analysis

The data of behavioral studies were evaluated by an analysis of variance one-way ANOVA followed by Bonferroni's post hoc test (statistical significance set at $p < 0.05$).

Declaration of competing interest

The authors declare that they have no known competing financial interests or personal relationships that could have appeared to influence the work reported in this paper.

Acknowledgments

Authors thank very much Ms. Luiza Wardzała, the master student for her effective participation in the synthesis within the Student Medicinal Chemistry Scientific Group at the Department of Technology and Biotechnology of Drugs, JU MC (Studenckie Koło Chemii Medycznej, UJCM). This study was supported by the National Science Center (Poland) Grant No. UMO-2018/31/B/NZ7/02160. The paper was written during doctoral studies of Ms. Kamila Buzun under the project № POWR.03.02.00-00-I051/16 co-funded from European Union funds, POW ER 2014–2020.

Appendix A. Supplementary data

Supplementary data to this article can be found online at https://doi.org/10.1016/j.ejmech.2020.112529.

References

[1] M. Ruat, E. Traiffort, J.M. Arrang, J. Tardivellacombe, J. Diaz, R. Leurs, J.C. Schwartz, A novel rat serotonin (5-HT6) receptor: molecular cloning, localization and stimulation of cAMP accumulation, Biochem. Biophys. Res. Commun. 193 (1993) 268–276, https://doi.org/10.1006/bbrc.1993.1619.

[2] D. Marazziti, S. Baroni, A. Pirone, G. Giannaccini, L. Betti, G. Testa, L. Schmid, L. Palego, F. Borsini, F. Bordi, I. Piano, C. Gargini, M. Castagna, M. Catena-Dell'Osso, A. Lucacchini, Serotonin receptor of type 6 (5-HT6) in human prefrontal cortex and hippocampus post-mortem: an immunohistochemical and immunofluorescence study, Neurochem. Int. 62 (2013) 182–188, https://doi.org/10.1016/j.neuint.2012.11.013.

[3] A. Wesołowska, Potential role of the 5-HT 6 receptor in depression and anxiety: an overview of preclinical data, Pharmacol. Rep. 62 (2010) 564–577, https://doi.org/10.1016/S1734-1140(10)70315-7.

[4] K. Wicke, A. Haupt, A. Bespalov, Investigational drugs targeting 5-HT6 receptors for the treatment of Alzheimers disease, Expet Opin. Invest. Drugs 24 (2015) 1515–1528, https://doi.org/10.1517/13543784.2015.1102884.

[5] B. Benhamú, M. Martín-Fontecha, H. Vázquez-Villa, L. Pardo, M.L. López-Rodríguez, Serotonin 5-HT6receptor antagonists for the treatment of cognitive deficiency in Alzheimer's disease, J. Med. Chem. 57 (2014) 7160–7181, https://doi.org/10.1021/jm5003952.

[6] S.E. Shortall, O.H. Negm, M. Fowler, L.C. Fairclough, P.J. Tighe, P.M. Wigmore,

M.V. King, Characterization of behavioral, signaling and cytokine alterations in a rat neurodevelopmental model for schizophrenia, and their reversal by the 5-HT6 receptor antagonist SB-399885, Mol. Neurobiol. 55 (2018) 7413–7430, https://doi.org/10.1007/s12035-018-0940-0.
[7] M. Kotańska, K. Lustyk, A. Bucki, M. Marcinkowska, J. Śniecikowska, M. Kołaczkowski, Idalopirdine, a selective 5-HT6 receptor antagonist, reduces food intake and body weight in a model of excessive eating, Metab. Brain Dis. 33 (2018) 733–740, https://doi.org/10.1007/s11011-017-0175-1.
[8] A. Frassetto, J. Zhang, J.Z. Lao, A. White, J.M. Metzger, T.M. Fong, R.Z. Chen, Reduced sensitivity to diet-induced obesity in mice carrying a mutant 5-HT6 receptor, Brain Res. 1236 (2008) 140–144, https://doi.org/10.1016/j.brainres.2008.08.012.
[9] S.M. Hagsäter, A. Lisinski, E. Eriksson, 5-HT6 receptor antagonism reduces defecation in rat: a potential treatment strategy for irritable bowel syndrome with diarrhea, Eur. J. Pharmacol. 864 (2019) 172718, https://doi.org/10.1016/j.ejphar.2019.172718.
[10] J. Rychtyk, A. Partyka, J. Gdula-Argasińska, K. Mysłowska, N. Wilczyńska, M. Jastrzębska-Więsek, A. Wesołowska, 5-HT6 receptor agonist and antagonist improve memory impairments and hippocampal BDNF signaling alterations induced by MK-801, Brain Res. 1722 (2019) 146375, https://doi.org/10.1016/j.brainres.2019.146375.
[11] A.M. Bokare, M. Bhonde, R. Goel, Y. Nayak, 5-HT6 receptor agonist and antagonist modulates ICV-STZ-induced memory impairment in rats, Psychopharmacology (Berlin) 235 (2018) 1557–1570, https://doi.org/10.1007/s00213-018-4866-z.
[12] The Study of a Selective 5-ht6 Receptor Antagonist, HEC30654AcOH,in Healthy Subjects - Full Text View - ClinicalTrials.gov, n.d, https://clinicaltrials.gov/ct2/show/NCT03655873?term=5-HT6&draw=2&rank=1. (Accessed 23 January 2020).
[13] T. Fullerton, B. Binneman, W. David, M. Delnomdedieu, J. Kupiec, P. Lockwood, J. Mancuso, J. Miceli, J. Bell, A Phase 2 clinical trial of PF-05212377 (SAM-760) in subjects with mild to moderate Alzheimer's disease with existing neuropsychiatric symptoms on a stable daily dose of donepezil, Alzheimer's Res. Ther. 10 (2018) 38, https://doi.org/10.1186/s13195-018-0368-9.
[14] Study evaluating intepirdine (RVT-101) in subjects with mild to moderate Alzheimer's disease on donepezil: MINDSET study - full text view - ClinicalTrials.gov, n.d, https://clinicaltrials.gov/ct2/show/NCT02585934?term=SB-742457&draw=2&rank=7. (Accessed 23 January 2020).
[15] Study evaluating the Safety,Tolerability, PK and PD of SAM-531 in the subjects with mild to moderate Alzheimer's disease - full text view - ClinicalTrials.gov, n.d, https://clinicaltrials.gov/ct2/show/NCT00481520?term=SAM-531&draw=2&rank=7. (Accessed 23 January 2020).
[16] Long-term safety and tolerability of idalopirdine (Lu AE58054) as adjunctive treatment to donepezil in patients with mild-moderate Alzheimer's disease - full text view - ClinicalTrials.gov, n.d, https://clinicaltrials.gov/ct2/show/NCT02079246?term=LU-AE58054&draw=2&rank=8. (Accessed 23 January 2020).
[17] A safety and efficacy study of oral dimebon in patients with mild-to-moderate Alzheimer's disease - full text view - ClinicalTrials.gov, n.d, https://clinicaltrials.gov/ct2/show/NCT00675623?term=PF+01913539&draw=3&rank=11. (Accessed 23 January 2020).
[18] Y.A. Ivanenkov, A.G. Majouga, M.S. Veselov, N.V. Chufarova, S.S. Baranovsky, G.I. Filkov, Computational approaches to the design of novel 5-HT6R ligands, Rev. Neurosci. 25 (2014) 451–467, https://doi.org/10.1515/revneuro-2014-0030.
[19] A.K. Chatterjee, Cell-based medicinal chemistry optimization of high-throughput screening (HTS) hits for orally active antimalarials. part 1: challenges in potency and absorption, distribution, metabolism, excretion/pharmacokinetics (ADME/PK), J. Med. Chem. 56 (2013) 7741–7749, https://doi.org/10.1021/jm400314m.
[20] C.L. Gentry, R.D. Egleton, T. Gillespie, T.J. Abbruscato, H.B. Bechowski, V.J. Hruby, T.P. Davis, The effect of halogenation on blood-brain barrier permeability of a novel peptide drug, Peptides 20 (1999) 1229–1238, https://doi.org/10.1016/s0196-9781(99)00127-8.
[21] G. Gerebtzoff, X. Li-Blatter, H. Fischer, A. Frentzel, A. Seelig, Halogenation of drugs enhances membrane binding and permeation, Chembiochem 5 (2004) 676–684, https://doi.org/10.1002/cbic.200400017.
[22] L. Mendez, G. Henriquez, S. Sirimulla, M. Narayan, Looking back, looking forward at halogen bonding in drug discovery, Molecules 22 (2017) 22–25, https://doi.org/10.3390/molecules22091397.
[23] J.A. González-Vera, R.A. Medina, M. Martín-Fontecha, A. Gonzalez, T. De La Fuente, H. Vázquez-Villa, J. García-Cárceles, J. Botta, P.J. McCormick, B. Benhamú, L. Pardo, M.L. López-Rodríguez, A new serotonin 5-HT 6 receptor antagonist with procognitive activity - importance of a halogen bond interaction to stabilize the binding, Sci. Rep. 7 (2017), https://doi.org/10.1038/srep41293.
[24] K. Marciniec, R. Kurczab, M. Książek, E. Bębenek, E. Chrobak, G. Satała, A.J. Bojarski, J. Kusz, P. Zajdel, Structural determinants influencing halogen bonding: a case study on azinesulfonamide analogs of aripiprazole as 5-HT1A, 5-HT7, and D2 receptor ligands, Chem. Cent. J. 12 (2018), https://doi.org/10.1186/s13065-018-0422-5.
[25] Y. Zhou, Y. Wang, P. Li, X.P. Huang, X. Qi, Y. Du, N. Huang, Exploring halogen bonds in 5-hydroxytryptamine 2B receptor-ligand interactions, ACS Med. Chem. Lett. 9 (2018) 1019–1024, https://doi.org/10.1021/acsmedchemlett.8b00300.
[26] R. Kurczab, V. Canale, G. Satała, P. Zajdel, A.J. Bojarski, Amino acid hot spots of halogen bonding: a combined theoretical and experimental case study of the 5-HT7 receptor, J. Med. Chem. 61 (2018) 8717–8733, https://doi.org/10.1021/acs.jmedchem.8b00828.
[27] R. Kurczab, K. Kucwaj-Brysz, P. Śliwa, The significance of halogen bonding in ligand–receptor interactions: the lesson learned from molecular dynamic simulations of the D4 receptor, Molecules 25 (2019) 91, https://doi.org/10.3390/molecules25010091.
[28] W. Ali, M. Więcek, D. Łażewska, R. Kurczab, M. Jastrzębska-Więsek, G. Satała, K. Kucwaj-Brysz, A. Lubelska, M. Głuch-Lutwin, B. Mordyl, A. Siwek, M.J. Nasim, A. Partyka, S. Sudoł, G. Latacz, A. Wesołowska, K. Kieć-Kononowicz, J. Handzlik, Synthesis and computer-aided SAR studies for derivatives of phenoxyalkyl-1,3,5-triazine as the new potent ligands for serotonin receptors 5-HT6, Eur. J. Med. Chem. 178 (2019) 740–751, https://doi.org/10.1016/j.ejmech.2019.06.022.
[29] R. Kurczab, W. Ali, D. Łazewska, M. Kotánska, M. Jastrzebska-Wiesek, G. Satała, M. Wiecek, A. Lubelska, G. Latacz, A. Partyka, M. Starek, M. Dabrowska, A. Wesołowska, C. Jacob, K. Kiéc-Kononowicz, J. Handzlik, Computer-aided studies for novel arylhydantoin 1,3,5-triazine derivatives as 5-HT6 serotonin receptor ligands with antidepressive-like, anxiolytic and antiobesity action in vivo, Molecules 23 (2018) 2529, https://doi.org/10.3390/molecules23102529.
[30] D. Łażewska, R. Kurczab, M. Więcek, G. Satała, K. Kieć-Kononowicz, J. Handzlik, Synthesis and computer-aided analysis of the role of linker for novel ligands of the 5-HT 6 serotonin receptor among substituted 1,3,5-triazinylpiperazines, Bioorg. Chem. 84 (2019) 319–325, https://doi.org/10.1016/j.bioorg.2018.11.046.
[31] D. Łażewska, R. Kurczab, M. Więcek, K. Kamińska, G. Satała, M. Jastrzębska-Więsek, A. Partyka, A.J. Bojarski, A. Wesołowska, K. Kieć-Kononowicz, J. Handzlik, The computer-aided discovery of novel family of the 5-HT6 serotonin receptor ligands among derivatives of 4-benzyl-1,3,5-triazine, Eur. J. Med. Chem. 135 (2017) 117–124, https://doi.org/10.1016/j.ejmech.2017.04.033.
[32] G. Latacz, A. Lubelska, M. Jastrzębska-Więsek, A. Partyka, M.A. Marć, G. Satała, D. Wilczyńska, M. Kotańska, M. Więcek, K. Kamińska, A. Wesołowska, K. Kieć-Kononowicz, J. Handzlik, The 1,3,5-triazine derivatives as innovative chemical family of 5-HT6 serotonin receptor agents with therapeutic perspectives for cognitive impairment, Int. J. Mol. Sci. 20 (2019) 1–21, https://doi.org/10.3390/ijms20143420.
[33] J.F. López-Giménez, J. González-Maeso, Hallucinogens and serotonin 5-HT2A receptor-mediated signaling pathways, in: Curr. Top. Behav. Neurosci, Springer Verlag, 2018, pp. 45–73, https://doi.org/10.1007/7854_2017_478.
[34] D.A. Sykes, H. Moore, L. Stott, N. Holliday, J.A. Javitch, J.R. Lane, S.J. Charlton, Extrapyramidal side effects of antipsychotics are linked to their association kinetics at dopamine D2 receptors, Nat. Commun. 8 (2017) 1–11, https://doi.org/10.1038/s41467-017-00716-z.
[35] N. Zareifopoulos, C. Papatheodoropoulos, Effects of 5-HT-7 receptor ligands on memory and cognition, Neurobiol. Learn. Mem. 136 (2016) 204–209, https://doi.org/10.1016/j.nlm.2016.10.011.
[36] X. Chen, A. Murawski, K. Patel, C.L. Crespi, P.V. Balimane, A novel design of artificial membrane for improving the PAMPA model, Pharm. Res. (N. Y.) 25 (2008) 1511–1520, https://doi.org/10.1007/s11095-007-9517-8.
[37] G. Latacz, A. Lubelska, M. Jastrzębska-Więsek, A. Partyka, A. Sobiło, A. Olejarz, K. Kucwaj-Brysz, G. Satała, A.J. Bojarski, A. Wesołowska, K. Kieć-Kononowicz, J. Handzlik, In the search for a lead structure among series of potent and selective hydantoin 5-HT $_7$ R agents: the drug-likeness in vitro study, Chem. Biol. Drug Des. 90 (2017) 1295–1306, https://doi.org/10.1111/cbdd.13106.
[38] G. Latacz, A. Lubelska, M. Jastrzębska-Więsek, A. Partyka, K. Kucwaj-Brysz, A. Wesołowska, K. Kieć-Kononowicz, J. Handzlik, MF-8, a novel promising arylpiperazine-hydantoin based 5-HT 7 receptor antagonist: in vitro drug-likeness studies and in vivo pharmacological evaluation, Bioorg. Med. Chem. Lett 28 (2018) 878–883, https://doi.org/10.1016/j.bmcl.2018.02.003.
[39] K. Socała, S. Mogilski, M. Pieróg, D. Nieoczym, M. Abram, B. Szulczyk, A. Lubelska, G. Latacz, U. Doboszewska, P. Wlaź, K. Kamiński, KA-11, a novel pyrrolidine-2,5-dione derived broad-spectrum anticonvulsant: its anti-epileptogenic, antinociceptive properties and in vitro characterization, ACS Chem. Neurosci. 10 (2019) 636–648, https://doi.org/10.1021/acschemneuro.8b00476.
[40] G. Latacz, A.S. Hogendorf, A. Hogendorf, A. Lubelska, J.M. Wierońska, M. Woźniak, P. Cieślik, K. Kieć-Kononowicz, J. Handzlik, A.J. Bojarski, Search for a 5-CT alternative. In vitro and in vivo evaluation of novel pharmacological tools: 3-(1-alkyl-1H-imidazol-5-yl)-1H-indole-5-carboxamides, low-basicity 5-HT7 receptor agonists, Medchemcomm 9 (2018) 1882–1890, https://doi.org/10.1039/c8md00313k.
[41] A. Lubelska, G. Latacz, M. Jastrzębska-Więsek, M. Kotańska, R. Kurczab, A. Partyka, M.A. Marć, D. Wilczyńska, A. Doroz-Płonka, D. Łazewska, A. Wesołowska, K. Kiéc-Kononowicz, J. Handzlik, Are the hydantoin-1,3,5-triazine 5-HT6R ligands a hope to a find new procognitive and anti-obesity drug? Considerations based on primary in vivo assays and ADME-tox profile in vitro, Molecules 24 (2019), https://doi.org/10.3390/molecules24244472.
[42] N.M.W.J. de Bruin, J. Prickaerts, A. van Loevezijn, J. Venhorst, L. de Groote, P. Houba, O. Reneerkens, S. Akkerman, C.G. Kruse, Two novel 5-HT6 receptor antagonists ameliorate scopolamine-induced memory deficits in the object recognition and object location tasks in Wistar rats, Neurobiol. Learn. Mem. 96 (2011) 392–402, https://doi.org/10.1016/j.nlm.2011.06.015.

[43] D. Łazewska, M. Więcek, J. Ner, K. Kamińska, T. Kottke, J.S. Schwed, M. Zygmunt, T. Karcz, A. Olejarz, K. Kuder, G. Latacz, M. Grosicki, J. Sapa, J. Karolak-Wojciechowska, H. Stark, K. Kieć-Kononowicz, Aryl-1,3,5-triazine derivatives as histamine H4 receptor ligands, Eur. J. Med. Chem. 83 (2014) 534–546, https://doi.org/10.1016/j.ejmech.2014.06.032.
[44] K. Kamińska, J. Ziemba, J. Ner, J.S. Schwed, D. Łazewska, M. Więcek, T. Karcz, A. Olejarz, G. Latacz, K. Kuder, T. Kottke, M. Zygmunt, J. Sapa, J. Karolak-Wojciechowska, H. Stark, K. Kieć-Kononowicz, (2-Arylethenyl)-1,3,5-triazin-2-amines as a novel histamine H4 receptor ligands, Eur. J. Med. Chem. 103 (2015) 238–251, https://doi.org/10.1016/j.ejmech.2015.08.014.
[45] E. Żesławska, W. Nitek, W. Tejchman, J. Handzlik, Influence of 3-{5-[4-(diethylamino)benzylidene]rhodanine}propionic acid on the conformation of 5-(4-chlorobenzylidene)-2-(4-methylpiperazin-1-yl)-3H-imidazol-4(5H)-one, Acta Crystallogr. Sect. C Struct. Chem. 74 (2018) 1427–1433, https://doi.org/10.1107/S2053229618013980.
[46] R. Kurczab, The evaluation of QM/MM-driven molecular docking combined with MM/GBSA calculations as a halogen-bond scoring strategy, Acta Crystallogr. Sect. B Struct. Sci. Cryst. Eng. Mater. 73 (2017) 188–194, https://doi.org/10.1107/S205252061700138X.
[47] K. Grychowska, R. Kurczab, P. Śliwa, G. Satała, K. Dubiel, M. Matłoka, R. Moszczyński-Pętkowski, J. Pieczykolan, A.J. Bojarski, P. Zajdel, Pyrroloquinoline scaffold-based 5-HT6R ligands: synthesis, quantum chemical and molecular dynamic studies, and influence of nitrogen atom position in the scaffold on affinity, Bioorg. Med. Chem. 26 (2018) 3588–3595, https://doi.org/10.1016/j.bmc.2018.05.033.
[48] M.C. Burla, R. Caliandro, B. Carrozzini, G.L. Cascarano, C. Cuocci, C. Giacovazzo, M. Mallamo, A. Mazzone, G. Polidori, Crystal structure determination and refinement via SIR2014, J. Appl. Crystallogr. 48 (2015) 306–309, https://doi.org/10.1107/S1600576715001132.
[49] G.M. Sheldrick, Crystal structure refinement with SHELXL, Acta Crystallogr. Sect. C Struct. Chem. 71 (2015) 3–8, https://doi.org/10.1107/S2053229614024218.
[50] C.F. Macrae, P.R. Edgington, P. McCabe, E. Pidcock, G.P. Shields, R. Taylor, M. Towler, J. van de Streek, Mercury IUCr, Visualization and analysis of crystal structures, J. Appl. Crystallogr. 39 (2006) 453–457, https://doi.org/10.1107/S002188980600731X.
[51] n.d, Schrödinger Release 2019-4, LigPrep, Schrödinger, LLC, New York, NY, 2019.
[52] n.d, Schrödinger Release 2019-4, Epik, Schrödinger, LLC, New York, NY, 2019.
[53] E. Harder, W. Damm, J. Maple, C. Wu, M. Reboul, J.Y. Xiang, L. Wang, D. Lupyan, M.K. Dahlgren, J.L. Knight, J.W. Kaus, D.S. Cerutti, G. Krilov, W.L. Jorgensen, R. Abel, R.A. Friesner, OPLS3: a force field providing broad coverage of drug-like small molecules and proteins, J. Chem. Theor. Comput. 12 (2016) 281–296, https://doi.org/10.1021/acs.jctc.5b00864.
[54] Schrödinger Release 2019-4: QM-Polarized Ligand Docking Protocol, Glide, Schrödinger, LLC, New York, NY, 2019. Jaguar, Schrödinger, LLC, New York, NY, 2019; QSite, Schrödinger, LLC, New York, NY, 2019., (n.d.).
[55] Y. Cheng, W.H. Prusoff, Relationship between the inhibition constant (K1) and the concentration of inhibitor which causes 50 per cent inhibition (I50) of an enzymatic reaction, Biochem. Pharmacol. 22 (1973) 3099–3108.
[56] A. Ennaceur, J. Delacour, A new one-trial test for neurobiological studies of memory in rats. 1: behavioral data, Behav, Brain Res. 31 (1988) 47–59, https://doi.org/10.1016/S0166-4328(05)80315-8.
[57] P. Zajdel, T. Kos, K. Marciniec, G. Satała, V. Canale, K. Kamiński, M. Hołuj, T. Lenda, R. Koralewski, M. Bednarski, L. Nowiński, J. Wójcikowski, W.A. Daniel, A. Nikiforuk, I. Nalepa, P. Chmielarz, J. Kuśmierczyk, A.J. Bojarski, P. Popik, Novel multi-target azinesulfonamides of cyclic amine derivatives as potential antipsychotics with pro-social and pro-cognitive effects, Eur. J. Med. Chem. 145 (2018) 790–804, https://doi.org/10.1016/j.ejmech.2018.01.002.